A TRIDENT SCHOLAR PROJECT REPORT

NO. 495

Advancing the Synthesis of Polyionic Biocomposite Materials by the Natural Fiber Welding Process

by

Midshipman 1/C Christian E. Hoffman, USN

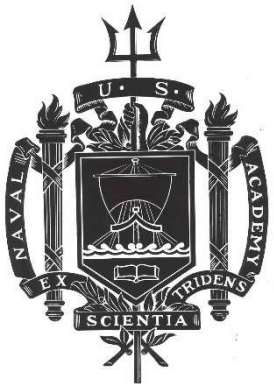

UNITED STATES NAVAL ACADEMY
ANNAPOLIS, MARYLAND

USNA-1531-2

REPORT DOCUMENTATION PAGE

Form Approved
OMB No. 0704-0188

1. REPORT DATE *(DD-MM-YYYY)*	**2. REPORT TYPE**	**3. DATES COVERED** *(From - To)*
7/6/20		

4. TITLE AND SUBTITLE
Advancing the Synthesis of Polyionic Biocomposite Materials by the Natural Fiber Welding Process

5a. CONTRACT NUMBER

5b. GRANT NUMBER

5c. PROGRAM ELEMENT NUMBER

6. AUTHOR(S)
Hoffman, Christian E.

5d. PROJECT NUMBER

5e. TASK NUMBER

5f. WORK UNIT NUMBER

7. PERFORMING ORGANIZATION NAME(S) AND ADDRESS(ES)

8. PERFORMING ORGANIZATION REPORT NUMBER

9. SPONSORING / MONITORING AGENCY NAME(S) AND ADDRESS(ES)
U.S. Naval Academy
Annapolis, MD 21402

10. SPONSOR/MONITOR'S ACRONYM(S)

11. SPONSOR/MONITOR'S REPORT NUMBER(S)
Trident Scholar Report no. 495 (2020)

12. DISTRIBUTION / AVAILABILITY STATEMENT

This document has been approved for public release; its distribution is UNLIMITED.

13. SUPPLEMENTARY NOTES

14. ABSTRACT

Biomaterials such as cotton and silk are abundant natural resources with material properties equal or superior to many synthetic polymers. Using ionic liquids (ILs) and the Natural Fiber Welding (NFW) process, biomaterials can be chemically and physically enhanced. Here we present progress on using polymerizable ionic liquids (Poly-ILs) in the NFW process. Poly-ILs with different cation and anion structures were synthesized and subsequently characterized using 1-H and 13-C NMR, then evaluated for their ability to (i) polymerize and (ii) solubilize a biopolymer (cellulose) matrix. The best performing Poly-ILs were used in the NFW process to prepare polyionic biocomposite materials.

15. SUBJECT TERMS
Polymerizable Ionic Liquids, Biopolymer, Natural Fiber Welding, Polymerization

16. SECURITY CLASSIFICATION OF:			**17. LIMITATION OF ABSTRACT**	**18. NUMBER OF PAGES**	**19a. NAME OF RESPONSIBLE PERSON**
a. REPORT	**b. ABSTRACT**	**c. THIS PAGE**		57	**19b. TELEPHONE NUMBER** *(include area code)*

U.S.N.A. --- Trident Scholar project report; no. 495 (2020)

ADVANCING THE SYNTHESIS OF POLYIONIC BIOCOMPOSITE MATERIALS BY THE NATURAL FIBER WELDING PROCESS

by

Midshipman 1/C Christian E. Hoffman
United States Naval Academy
Annapolis, Maryland

_____
(signature)

Certification of Adviser(s) Approval

CDR David P. Durkin, USN
Chemistry Department

_____
(signature)

_____
(date)

Professor Paul C. Trulove
Chemistry Department

_____
(signature)

_____
(date)

Acceptance for the Trident Scholar Committee

Professor Maria J. Schroeder
Associate Director of Midshipman Research

_____
(signature)

_____
(date)

USNA-1531-2

1. Abstract

Biomaterials such as cotton and silk are abundant natural resources with mechanical properties that can exceed those of synthetic polymers. However, current industrial processing methods degrade the structure of the biomaterial and utilize pollutants such as carbon disulfide. As an alternative processing technique, biomaterials can be chemically and physically enhanced using ionic liquids (ILs) via Natural Fiber Welding (NFW). NFW is an environmentally-friendly process that entails the controlled manipulation and enhancement of biomaterials by adjusting variables such as IL concentration, welding temperature, and exposure time.

The purpose of this study is to develop the NFW process for making polyionic biocomposites out of biopolymer materials and polymerizable ionic liquids (Poly-ILs). A variety of Poly-ILs with differing cation and anion pairs have been synthesized and characterized using nuclear magnetic resonance (NMR) and attenuated total reflection infrared spectroscopy (ATR-IR). Poly-ILs were evaluated for their ability to polymerize and act as NFW solvents. Polymerization was conducted with photo- and thermal initiators at varying temperatures and initiation times. Polymerized Poly-ILs were characterized with ATR-IR and Raman spectroscopy. NFW solvent suitability was determined by treating cotton yarns with neat Poly-ILs and co-solvent mixtures. IL-treated yarns were characterized using scanning electron microscopy (SEM) and/or optical microscopy.

This report highlights advancements made in synthesizing Poly-ILs, conducting ex-situ polymerization experiments, treating cotton substrates with novel Poly-ILs, and preparing polyionic biocomposites via NFW. Four of the synthesized Poly-ILs with imidazolium-based cations and trifluoroacetate, thiocyanate, or alkylphosphonate anions demonstrated suitable properties for the desired application. 1-ethyl-3-vinylimidazolium ethylphosphonate (EVIEPhos) and 1-methyl-3-vinylimidazolium methylphosphonate (MVIMPhos) were studied most closely. Welded polyionic biocomposites prepared from EVIEPhos and MVIMPhos were evaluated using microscopy and spectroscopy to reveal the degree of polymerization and welding.

2. Keywords

Polymerizable Ionic Liquids, Biopolymer, Natural Fiber Welding, Polymerization

3. Acknowledgements

"Science is a team sport, we're all family." These words have become the embodiment of my research experiences over the last two years. Being a member of the Trulove/Durkin lab group has provided me with incredible challenges, fascinating insights, and the occasional success. None of which would be possible alone. I've been so very lucky to be part of such an incredible family.

To Ashlee, I'm very happy the chaotic lunch in King Hall didn't create any doubts about joining the group. I'm even more thankful that you always push me to think deeper about a topic. Your insightful questions frequently made me rethink my perceptions and led me to a better view of the larger picture.

To Tyler, I'll always appreciate the effort and assistance you provided. Without your generous help I would never learn the intricacies of burning epoxy with Raman lasers, painstakingly pulling apart IR microscopes or how to correctly fumble with potentiostat leads. Whether solving problems with unique 3D printed jigs, testing out your fascinating demos for your plebe chemistry class or sharing a hearty laugh in the lab I'll miss working beside you in MI-250.

To CDR Durkin, while your mantra may have started as "A clean lab and a good notebook are all that matter" your actions have showed me that there is much more to research than what happens in the lab. You've always provided great advice on topics ranging from my development as a naval officer to creating the next hit chemistry song. One of the best parts of my day at USNA was coming into lab and getting a fist-bump or a big smile to get me ready for the day's experiments.

To Prof. Trulove, thank you for bringing me into such an incredible group. You've always pushed me to grow, both as a chemist and officer. Some of my greatest lessons were walking into your office to present what I thought were 'definitive' results and walking out with the reminder that there is always another piece of the puzzle to explore. While I may have missed out on our group hikes (I'll make it someday!!) I'll miss the adventures within the lab that always occurred when it came time for spring cleaning or organizing.

Outside of the incredible research family, I'd like to thank my Varsity Offshore Sailing Team family. While many of you will probably never read this, I'd like give my thanks for understanding why I am habitually sweaty when I show up to practice as I race to wrap up my experiments and speed walk to Robert Crown. It's been one of my life's great honors to lead the team and continue to pursue my passions off the water.

Finally, to my family, Mom, Dad, Ethan, and Collin. Thank you! Your never ending support for me has enabled me to push through tough days in the lab and days of leave filled with writing proposals and reports. While I may be the target of a couple 'chem-splaining' jokes around the dinner table, I wouldn't have it any other way.

4. Table of Contents

5. Introduction

Biomaterials (e.g., cotton, wood, silk) are abundant natural resources formed from biopolymers (e.g., cellulose, lignocellulose, silk proteins) that were the primary textile and manufacturing material until the introduction of synthetic polymers such as Bakelite[1] and nylon[2]. However, these natural biomaterials often have mechanical properties (e.g., stiffness, strength, extensibility, toughness) exceeding those of synthetic polymer materials such as Kevlar[3-6]. The superior mechanical properties are derived from the complex native structure of the material. Current industrial methods for processing biomaterials alters the innate morphology of the biomaterials and use toxic solvents such as carbon disulfide[7-8]. The result of these processes are materials with degraded mechanical properties and the release of hazardous byproducts. Previous research conducted by our laboratory has focused on enhancing the chemical and physical properties of biopolymer materials, particularly cotton, using a patented and environmentally-friendly process, termed Natural Fiber Welding (NFW), that enables the controlled manipulation of native biopolymer materials using ionic liquids (ILs)[9-11]. This report discusses our progress towards creating polyionic biocomposites via the NFW process using polymerizable ionic liquids (Poly-ILs) and evaluating the material's physicochemical properties.

Biomaterials have complex, highly ordered, structures that form during the natural synthesis process. The superior mechanical properties of biomaterials originate from this complex structure. Degrading any portion of the structure leads to the deterioration of mechanical properties. The NFW process enables the controlled manipulation of biomaterials and their structure without significantly degrading their material properties[12]. In cotton, there is a hierarchical structure consisting of a micro-, meso-, and macrostructure (Figure 1)[12]. The microstructure of cotton is comprised of cellulose I chains interconnected with hydrogen bonds and van der Waals forces. Localized organization of these cellulose chains forms ordered crystalline domains which comprise the mesostructures. Together, these formations create identifying features (macrostructures) such as the primary and secondary cell wall and a central void, called the lumen.

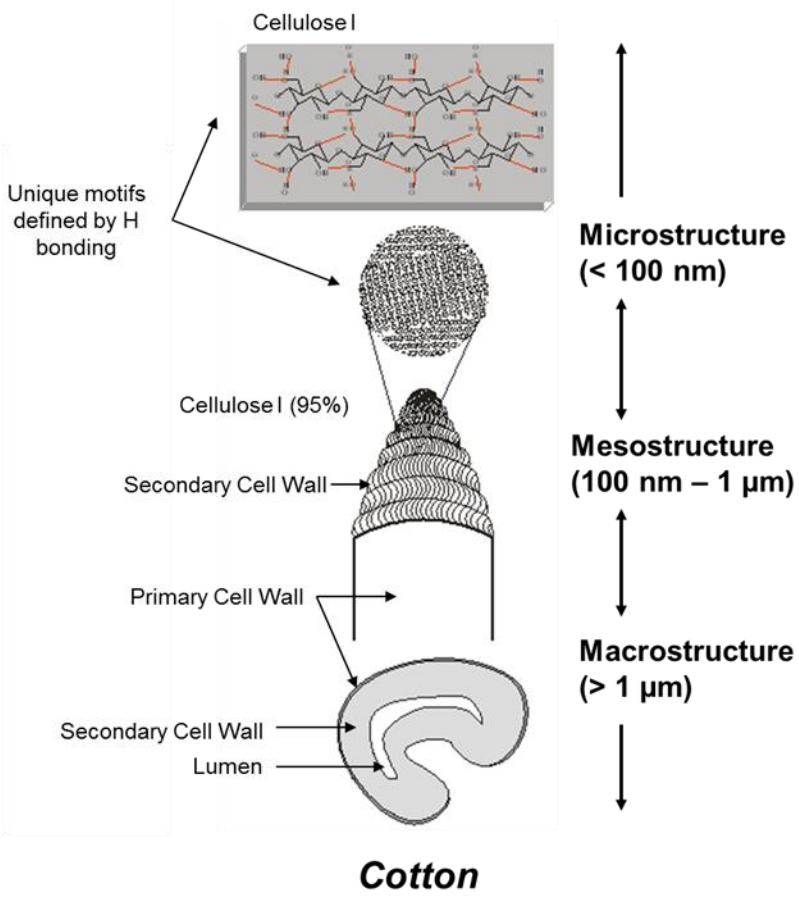

Figure 1. Micro-, meso-, and macro-, structure of Cotton.

Ionic liquids (IL) are nonvolatile, low melting point salts (typically < 100 °C)[13-14]. The low melting point of ILs is cause by weak-intermolecular interactions between the cation and anion pair, as well as the inability for the pair to stack well in a crystalline structure[15]. Altering the cation/anion combinations produces ILs with unique physical and chemical properties that can be exploited for a variety of applications including environmentally-friendly purifiers[16], lubricants[17], and solvents for biomaterials[7]. Polymerizable ionic liquids (Poly-ILs) are ILs that contain an alkenyl functional group, such as a vinyl (-CH=CH_2) or allyl (-CH_2-CH=CH_2), in the cation or anion structure (Figure 2). These functional groups can undergo controlled radical chain growth polymerization with heat (i.e., thermal initiation), or UV irradiation (i.e., photoinitiation) using radical initiators[18-19].

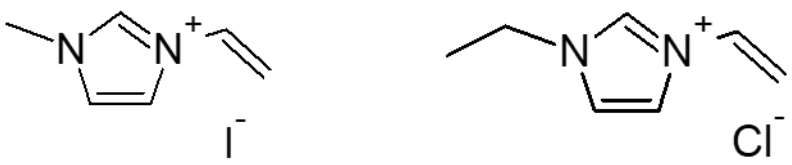

(a) **(b)**

Figure 2. Structures of some previously studied polymerizable ionic liquids, (a) 1-methyl-3-vinylimidazolium iodide (MVII) and (b) 1-ethyl-3-vinylimidazolium chloride (EVICl).

Extensive research has been conducted on the use of ILs to solubilize biomaterials such as silk[20-22] and cotton[7, 13, 23-24]. The manipulation of these natural materials to further enhance their mechanical properties has been accomplished using ILs in a process called Natural Fiber Welding (NFW)[9-10, 12]. The NFW process controls the dissolution of biopolymers through careful regulation of IL concentration, exposure time, and environmental conditions (Figure 3). Upon contacting a biomaterial substrate, the chaotropic cations and anions of the IL disrupt both the intra- and inter-molecular van der Waals forces between individual biopolymer chains. Disrupting these bonding forces enables the mobilization of the biopolymer. The degree of mobilization is dependent upon the interaction time between the biopolymer and IL and viscosity of the IL. Longer welding times and less viscous ILs enable a greater biopolymer mobilization. When the IL is removed from the biopolymer with a solvent (e.g., water, methanol, acetone), a process termed ‘quenching’, the van der Waals forces within and between biopolymer strands reform. The result of the NFW process is a redistributed biopolymer matrix that has enhanced physical and chemical properties[25].

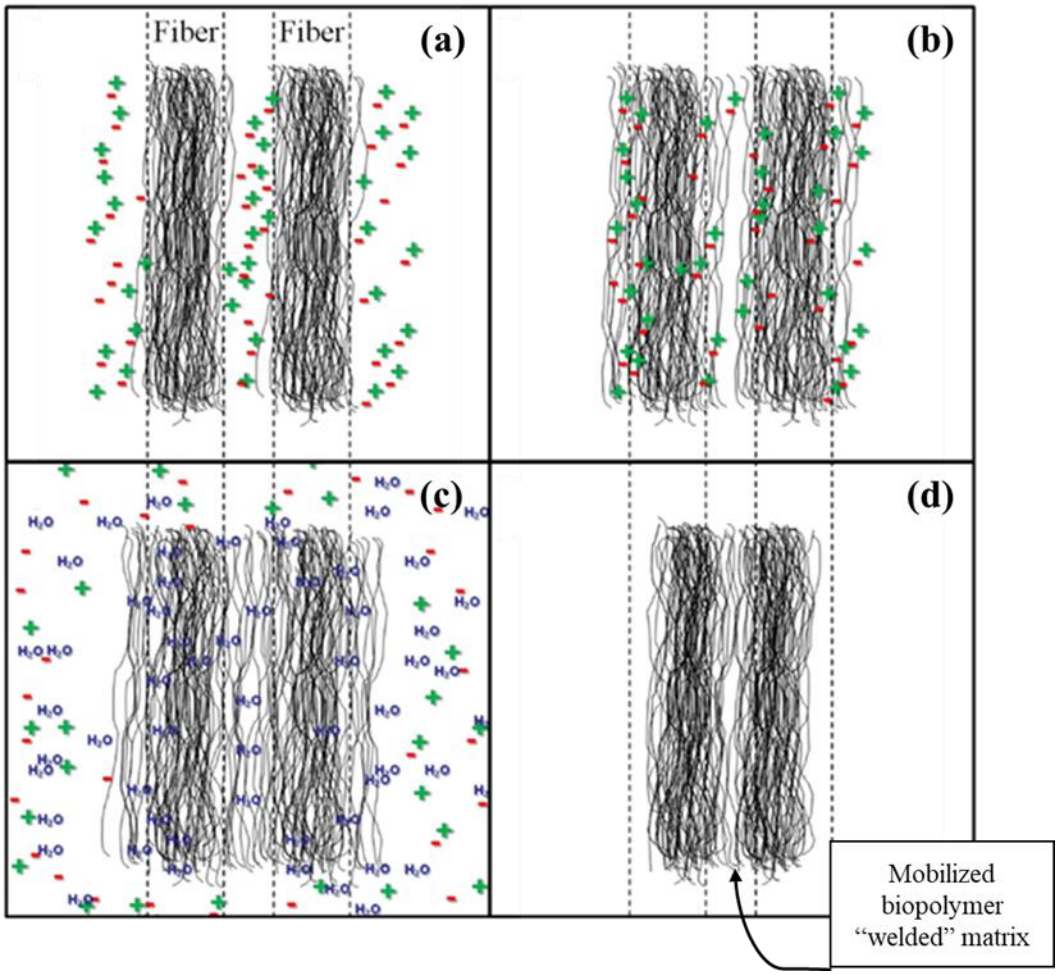

Figure 3. General visualization of NFW process on two fibers, (a) Adjacent fibers immediately after introduction of an IL. (b) Mobilization of the outer biopolymer layers in each fiber due to interactions with the IL. (c) Removal of IL by solvent rinse. (d) Welding of the two adjacent fibers following solvent removal via drying.

An alternative quenching process is possible when using Poly-ILs in the NFW process. Polymerizing Poly-ILs during NFW creates a cation or anion polymer chain that inhibits disruption of the van der Waals forces and limits further mobilization of the biopolymer. In-situ polymerization also retains the Poly-IL within the biopolymer matrix, potentially providing enhanced chemical properties, such as charged species mobilization.

Previous work in our group has successfully demonstrated the ability for certain Poly-ILs to act as NFW solvents while retaining their ability to polymerize.[11, 26] This prior work resulted in the synthesis of rudimentary polyionic biocomposites which required welding times of 3 hours and temperatures of 100 °C, conditions that are not optimal for timely and energy-efficient synthesis. Further work was also needed to exercise control over the polymerization process. The scope of the present work is focused on optimizing Poly-IL composition (cation and anion) to facilitate controlled polymerization, shorter welding times, and lower welding temperatures during the

synthesis of polyionic biocomposites. This report outlines our recent efforts using a series of novel Poly-ILs. Poly-ILs were synthesized and characterized before undergoing evaluation for their ability to polymerize and act as a NFW solvent. Poly-ILs that met both of these criteria were further investigated for their ability to prepare polyionic biocomposites. The structure and morphology of synthesized polyionic biocomposites were evaluated via scanning electron and optical microscopies.

6. Experimental

6.1 Materials

Cotton yarn (white, 100% cotton, mercerized, Coats Cotton), microcrystalline cellulose (MCC, Sigma), vinyl/acrylic copolymer filter disk (0.45 μm, DM Metrical Membranes), and polyvinylidene fluoride filter disk (PVDF, 0.22 μm, Durapore) were used as received. The following chemicals were used as received: potassium thiocyanate (98.5%, Fischer Chemical); deuterium oxide (99.8%, Acros Organics); dimethyl sulfoxide (DMSO-d_6, 99.9%, Sigma Aldrich); 1-chlorohexane (99%, Aldrich); acetonitrile (ACN, 99.8%, Sigma-Aldrich); 2-hydroxy-2-methylpropiophenone (HMPP, 97%, Sigma-Aldrich); methanol (99%, Pharmco-Aaper); 2,6-di-tert-buytl-4-methylphenol (BHT, 99%, Aldrich); azobisisobutyronitrile (AIBN, 98%, Sigma-Aldrich); potassium persulfate (99%, Sigma-Aldrich); ammonium benzoate (98%, Aldrich); sodium hydroxide pellets (98.8%, Fisher); potassium chloride (KCl, 99%, Sigma-Aldrich); calcium chloride ($CaCl_2$, 96%, Fisher Scientific), chloroform-*d* (99.8%, Acros Organics); and tetrahydrofuran (THF, 99%, Sigma-Aldrich). Dimethyl phosphite (98%, Sigma-Aldrich); diethyl phosphite (98%, Sigma-Aldrich), and 1-vinylimidazole (99%, Aldrich) were distilled before conducting alkylation reactions. All aqueous solutions were prepared using ultrapure water (Barnstead E-pure filtration system) with resistivity of > 18 MΩ cm^{-1}.

6.2 Material synthesis and procedures

6.2.1 Synthesis of polymerizable ionic liquids (Poly-ILs)

Ten Poly-ILs were synthesized during this study (Figure 4). Five of the Poly-ILs: 1-methyl-3-vinylimidazolium methylphosphonate (MVIMPhos), 1-ethyl-3-vinylimidazolium ethylphosphonate (EVIEPhos), 1-ethyl-3-vinylimidazolium chloride (EVIBr), 1-butyl-3-vinylimidazolium chloride (BVICl), and 1-hexyl-3-vinylimidazolium chloride (HVICl) were synthesized via the alkylation of 1-vinylimidazole with a dialkylphosphite or an alkyl halide (Figure 5a). Additional Poly-ILs with thiocyanate, trifluoroacetate, and benzoate anions were synthesized via mass action ion exchange (Figure 5b) or metathesis reaction (Figure 5c) from a corresponding 1-ethyl-3-vinylimidazolium bromide (EVIBr), EVICl or BVICl precursor.

Mass-action ion exchange was conducted using an anion exchange resin (IRA400, Alfa Aesar). Before each synthesis the anion exchange resin capacity was regenerated by eluting 4 L of 1.5 M sodium hydroxide (NaOH) through the column. The columns were then charged with a molar excess (1.5 M, 4 L) of the product anion, which exchanged with the hydroxide on the resin beads via mass action. The extent of charging was checked regularly by monitoring the pH of the column eluent with pH paper. The eluent of a regenerated column typically had a pH of ~12. When the

hydroxide anion was exchanged and completely rinsed with ultrapure water, the pH of the eluent would be approximately neutral.

Metathesis reactions were conducted by mixing a solution of precursor Poly-IL with the ammonium salt of a desired anion. For example, a solution of BVICl was mixed with ammonium trifluoroacetate to synthesize 1-butyl-3-vinylimidazolium trifluoroacetate (BVITFAc). Reactions were conducted in ACN at ambient temperature under N_2. Metathesis reactions resulted in a liquid Poly-IL and an insoluble ammonium chloride by-product. After filtering out the ammonium chloride, residual ACN was removed under reduced pressure with rotary evaporation to produce a neat Poly-IL.

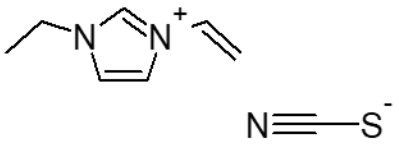

1-ethyl-3-vinylimidazolium thiocyanate
EVISCN

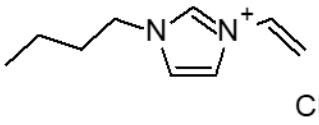

1-butyl-3-vinylimidazolium chloride
BVICl

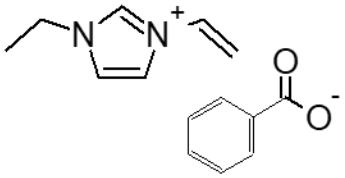

1-ethyl-3-vinylimidazolium benzoate
EVI(benzoate)

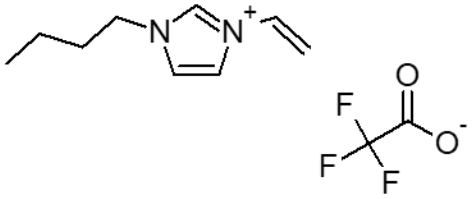

1-butyl-3-vinylimidazolium trifluoroacetate
BVITFAc

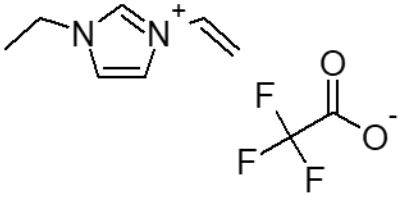

1-ethyl-3-vinylimidazolium trifluoroacetate
EVITFAc

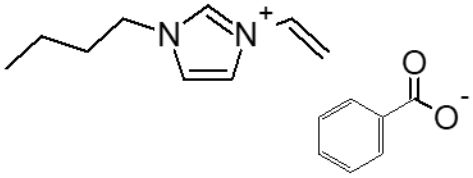

1-butyl-3-vinylimidazolium benzoate
BVI(benzoate)

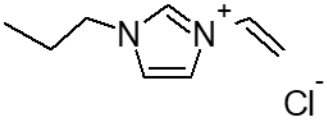

1-propyl-3-vinylimidazolium chloride
PVICl

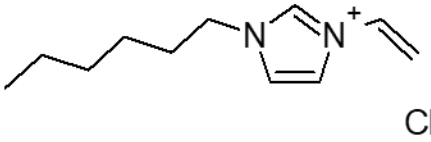

1-hexyl-3-vinylimidazolium chloride
HVICl

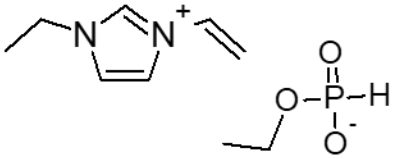

1-ethyl-3-vinylimidazolium ethylphosphonate
EVIEPhos

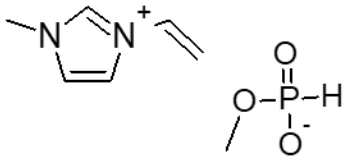

1-methyl-3-vinylimidazolium methylphosphonate
MVIMPhos

Figure 4. Poly-ILs synthesized in this study

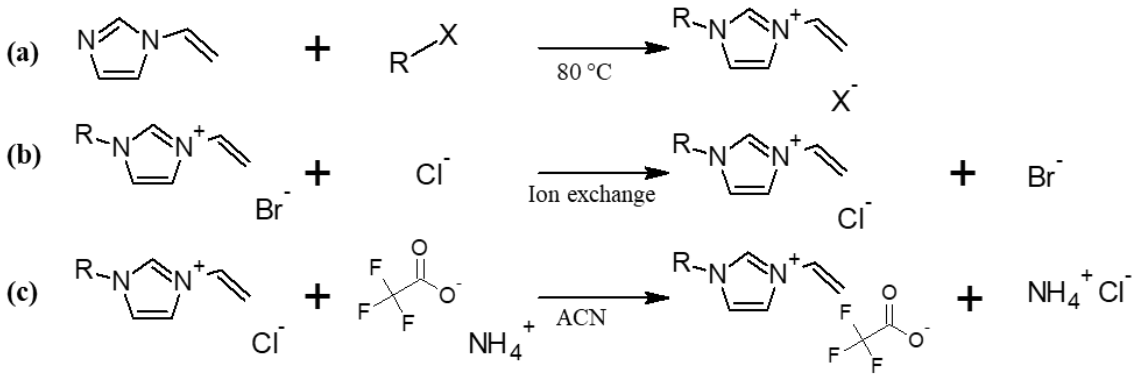

Figure 5. Reaction mechanism for synthesis of novel Poly-ILs, (a) alkylation of 1-vinylimidazole, (b) mass-action ion exchange, (c) metathesis reaction.

6.2.1.1 Synthesis of 1-ethyl-3-vinylimidazolium chloride (EVIBr) precursor

A solution of 1-bromoethane:1-vinylimidazole (2:1 mole ratio) in 10% (v/v) ACN was prepared. The solution was stirred vigorously at 30-40 °C for ca. 14 days. Excess reactants were decanted and the remaining ACN:EVIBr solution was added dropwise to stirring ethyl acetate, producing an EVIBr precipitate. The ethyl acetate:EVIBr mixture was transferred to a dry N_2 atmosphere glovebox. The EVIBr was collected via vacuum filtration and dried under vacuum. Analogous 1-alkyl-3-vinylimidazolium halide precursors (i.e., EVICl and BVICl) were prepared in a similar manner.

6.2.1.2 Synthesis of 1-ethyl-3-vinylimidazolium thiocyanate (EVISCN)

A solution of potassium thiocyanate was passed through an ion exchange column to charge the resin with thiocyanate anion. Additional ultrapure water was eluted through the column until the pH was approximately neutral. An EVIBr solution was prepared in ultrapure water and sonicated for 5 min. The EVIBr solution was then eluted through the thiocyanate-charged column with excess ultrapure water at a rate of ca. 1 mL/min. The eluent was collected for 48 hr and the water was removed under reduced pressure via rotary evaporation. The resulting solution was placed on a vacuum line for one week to dry the IL further. The resulting EVISCN was transferred to a dry N_2 glovebox and subsequently characterized using ^{1}H NMR in D_2O (Figure A-1).

6.2.1.3 Synthesis of 1-ethyl-3-vinylimidazolium trifluoroacetate with BHT inhibitor (EVITFAc)

A solution of ammonium trifluoroacetate was passed through an ion exchange column to charge the resin with trifluoroacetate anion. A solution of EVIBr was prepared in ultrapure water and sonicated for 5 min. The EVIBr solution was then eluted through the trifluoroacetate-charged column with excess ultrapure water at a rate of ca. 1 mL/min. The eluent was collected into a solution containing dibutylhydroxytoluene (BHT) (0.1 mole% with respect to the EVITFAc) to prevent auto-polymerization. The eluent was collected and the water was removed under reduced pressure via rotary evaporation. The resulting solution was placed on a vacuum line for one week to dry the IL further. The resulting EVITFAc with BHT was transferred into a dry N_2 atmosphere glovebox and subsequently characterized using ^{1}H NMR in D_2O (Figure A-2).

6.2.1.4 Synthesis of 1-ethyl-3-vinylimidazolium benzoate (EVI(benzoate)) via anion exchange

A solution of sodium hydroxide was passed through an ion exchange column to charge the resin with hydroxide anion. A solution of EVIBr was prepared in ultrapure water and sonicated for 5 min. The EVIBr solution was then eluted through the hydroxide-charged column to synthesize EVIOH. Initial eluent pH was approximately ~6.5-7 and became ~13 near the end of the collection. The collected solution was heated to ~40-50 °C and titrated with benzoic acid. This EVI(benzoate) solution was placed on a vacuum line for one week for further drying. ATR-IR of the EVI(benzoate) indicated the presence of benzoic acid. Additional ultrapure water was added to the solution to precipitate residual benzoic acid and the solution was filtered with a 0.45 μm vinyl/acrylic copolymer filter disk. The EVI(benzoate) filtrate was cooled to precipitate any remaining benzoic acid. The solution was filtered again and excess water was removed under reduced pressure via rotary evaporation.

6.2.1.5 Synthesis of 1-propyl-3-vinylimidazolium with BHT inhibitor (PVICl)

A solution of 1-chloropropane:1-vinylimidazole (2:1 mole ratio) and BHT (0.1 mole% with respect to the 1-vinylimidazole) in 10% (v/v) ACN was prepared in a pressure bottle. The solution was stirred vigorously at 30-40 °C for ca. 30 days. After refluxing, phase separation was observed between a light amber solution of crude PVICl and a clear solution of excess reactants. Excess reactants were removed under reduced pressure via rotary evaporation. The PVICl could not be recrystallized (in ethyl acetate), therefore the PVICl solution was placed on a vacuum line to dry for one week before being transferred to a dry N_2 atmosphere glovebox and subsequently characterized using ^{1}H NMR in D_2O (Figure A-3).

6.2.1.6 Synthesis of 1-butyl-3-vinylimidazolium chloride (BVICl)

A solution of 1-chlorobutane:1-vinylimidazole (2:1 mole ratio) was prepared and refluxed in ca. 5% (v/v) ACN for ca. 23 days at 80 °C. After refluxing, phase separation was observed between a dark amber solution of BVICl and a clear solution of excess reactants. Excess reactants were decanted from the reaction flask and the BVICl solution was transferred to a separatory funnel. The BVICl solution was slowly passed into ethyl acetate, producing a BVICl precipitate. The ethyl acetate:BVICl solution was stirred for 24 hr before being transferred to a dry N_2 atmosphere glovebox. The BVICl precipitate was collected via vacuum filtration and dried under vacuum in the N_2 glovebox for another two days. BVICl was characterized using ^{1}H NMR in D_2O (Figure A-4).

6.2.1.7 Synthesis of 1-hexyl-3-vinylimidazolium chloride (HVICl)

A solution of 1-chlorohexane:1-vinylimidazole (2:1 mole ratio) was prepared with ca. 5% (v/v) ACN and refluxed for ca. 40 days at ca. 30 °C. After one week, phase separation was observed between an opaque white solution of HVICl and clear solution of excess reactants. Reaction progress was monitored by characterization of the excess reactant phase using ^{1}H NMR in $CDCl_3$. The HVICl could not be recrystallized (in ethyl acetate, toluene, or hexane) and was transferred to a dry N_2 atmosphere glovebox for further evaluation.

6.2.1.8 Synthesis of 1-butyl-3-vinylimidazolium trifluoroacetate with BHT inhibitor (BVITFAc)

A solution of BVICl:ammonium trifluoroacetate (2 mole% excess ammonium trifluoroacetate) was prepared in ACN with BHT (0.1 mole% with respect to the BVICl). The solution was a light-yellow amber color and stirred under N_2 for 4 days. After 4 days, the solution was an opaque yellow color with a fine white precipitate at the bottom of the reaction flask. The solution was vacuum filtered twice through Millipore Durapore 0.22 μm PVDF filters to produce a clear yellow filtrate. After filtration, the BVITFAc solution was treated with neutral alumina for 2 days. The neutral alumina was removed via vacuum filtration using a Millipore Durapore 0.22 μm PVDF filter and excess ACN was removed under reduced pressure via rotary evaporation. The final BVITFAc solution was transferred to a dry N_2 atmosphere glovebox as a clear yellow room temperature liquid and characterized using ^{1}H NMR in DMSO-d_6 (Figure A-5).

6.2.1.9 Synthesis of 1-butyl-3-vinylimidazolium benzoate (BVI(benzoate))

A solution of BVICl:ammonium benzoate (2 mole% excess ammonium benzoate) was prepared in ACN. The solution was stirred at room temperature under N_2 for 14 days before undergoing vacuum filtration through a Millipore Durapore 0.22 μm PVDF filter. The filtrate was treated with neutral alumina for one day. The neutral alumina was removed via vacuum filtration using a Millipore Duraport 0.22 μm PVDF filter and excess ACN was removed under reduced pressure via rotary evaporation. The resulting BVI(benzoate) solution placed on a vacuum line to dry for one week before being transferred to a dry N_2 atmosphere glovebox for further evaluation.

6.2.1.10 Synthesis of 1-ethyl-3-vinylimidazolium ethylphosphonate (EVIEPhos)

A solution of 1-vinylimidazole:diethylphosphite (10 mole% excess of diethylphosphite) was prepared in ca. 50% (v/v) dry tetrahydrofuran (THF). The solution was refluxed under N_2 for 21 days. Excess THF was removed under reduced pressure via rotary evaporation. The EVIEPhos solution was placed on a vacuum line to dry for 7 days, then transferred into a dry N_2 atmosphere glovebox as reddish amber liquid and characterized using ^{1}H NMR in DMSO-d_6 (Figure A-6).

6.2.1.11 Synthesis of 1-methyl-3-vinylimidazolium methylphosphonate (MVIMPhos)

A solution of 1-vinylimidazole:dimethylphosphite (10 mole% excess of dimethylphosphite) was prepared in ca. 50% (v/v) dry THF in accordance with procedures by Fukaya *et al.*[27] The solution was refluxed and stirred under N_2 for two days. Excess THF was removed under reduced pressure via rotary evaporation. The resulting MVIMPhos solution was transferred to a separatory funnel, and rinsed with ethyl ether three times to remove any excess reactant. Ethyl ether was removed under reduced pressure via rotary evaporation. The MVIMPhos was placed on a vacuum line to dry for 7 days, then transferred into a dry N_2 atmosphere glovebox as an amber room-temperature liquid and characterized using ^{1}H NMR in DMSO-d_6 (Figure A-7).

6.2.2 Ex-situ Polymerization of Poly-ILs

6.2.2.1 Photo-initiated Polymerization of Poly-ILs

Solutions of EVISCN, EVITFAc, EVIEPhos, and MVIMPhos were polymerized via radical chain growth polymerization using HMPP photoinitiator. Solutions of EVISCN, EVITFAc, EVIEPhos, and MVIMPhos with various mole% of HMPP were prepared and irradiated with a

120V/100W mercury vapor lamp (Evergreen Pet Supplies) for times ranging from 3 min to 1 hr. This procedure was repeated for neat Poly-IL samples, Poly-IL solutions containing 3 wt% MCC, and samples that had undergone microwave NFW treatment. Polymerized products of neat Poly-ILs were dissolved in DMSO-d_6 and characterized using ^{1}H-NMR and Raman spectroscopy.

6.2.2.2 Thermal-Initiated Polymerization of Poly-ILs

Solutions of EVIEPhos and MVIMPhos were polymerized via radical chain growth polymerization with AIBN and potassium persulfate thermal initiators. Potassium persulfate was added neat to the Poly-ILs while AIBN required a co-solvent to dissolve into solution. Both initiators were added in 1 mole% concentrations with respect to the Poly-IL. Samples of the solutions were then initiated by heating at temperatures ranging from 60 °C to 100 °C for times ranging from 5 min to 1 hr. The polymerized products were characterized using ATR-IR spectroscopy. Raman spectroscopy was attempted, but unsuccessful because the polymerized samples emitted a large amount of fluorescence during analysis.

6.2.3 Poly-IL Welding Experiments

6.2.3.1 EVISCN Welding Experiments

A novel procedure for using EVISCN as an NFW solvent was tested using a CEM MARS5 microwave[7, 9, 12]. Cotton yarns were exposed to an excess of EVISCN in a test tube and placed within a microwave vessel. The vessel was exposed to a variety of power settings ranging from 140W to 300W for times ranging from 90 sec to 10 min. After microwaving, welding was quenched by rinsing the cotton yarns with methanol and placing them in an ultrapure water bath for 24 hr. Yarns were subsequently dried in a 60 °C oven for 24 hr. The yarns were characterized using SEM (Tescan Mira3) and high-resolution optical microscope (Zeiss Axio Imager).

6.2.3.2 EVITFAc Welding Experiments

An EVITFAc:ACN solution (1:1 mole ratio) was prepared in the glovebox. Cotton yarns were heated to 60 °C and exposed to the EVITFAc:ACN solution for 100 min. Welding was quenched using a methanol rinse before the samples were transferred to an ultrapure water bath for 24 hr. Samples were dried in a 60 °C oven for 24 hr before being characterized with a high-resolution optical microscope.

6.2.3.3 EVIEPhos Welding Experiments

Neat EVIEPhos and a solution of EVIEPhos:1 mole% HMPP were heated to 90 °C for five min. Aliquots of each liquid were deposited onto cotton yarns arranged in parallel and perpendicular orientations. Treatment lasted for 60 min at 90 °C before welding was quenched via methanol rinse for the neat EVIEPhos treated yarns and UV irradiation (30 min) for the EVIEPhos:HMPP treated yarns. Yarns treated with neat EVIEPhos were then rinsed in ultrapure water for 24 hr before drying in a 60 °C oven for 24 hr. Following drying, neat EVIEPhos treated yarns were cross-sectioned, gold sputter coated, and analyzed via SEM.

6.2.3.4 MVIMPhos Welding Experiments

Cotton yarns were wetted with MVIMPhos at 92 °C for treatment times of 10, 20, and 30 min. Welding was quenched with a methanol rinse. The treated yarns were then rinsed in ultrapure

water for 24 hr before drying in at 60 °C for 24 hr. After drying, the yarns were potted in epoxy, cross-sectioned using a microtome, and characterized using Raman spectroscopy.

6.3 Instrumental Methods

6.3.1 Nuclear Magnetic Resonance Spectroscopy (NMR)

^{1}H and ^{13}C NMR spectroscopy was conducted using a JEOL 400 MHz Spectrometer with JEOL Delta software. NMR spectroscopic analysis was utilized to monitor synthesis progress and assess the ultimate purity the Poly-ILs. In addition, NMR was used to evaluate the extent of polymerization of the Poly-ILs after initiation. To perform NMR measurements the neat and polymerized Poly-ILs were dissolved in either DMSO-d_6, $CDCl_3$, or D_2O.

6.3.2 Attenuated Total Reflection Fourier Transform Infrared Spectroscopy (ATR-IR)

ATR-IR spectra were collected using a Thermo Scientific Nicolet iS50 FTIR spectrometer. Spectral analysis was conducted using Thermo Scientific's OMNIC software.

6.3.3 Raman Spectroscopy

Raman spectroscopy was conducted using a Renishaw inVia Qontor confocal Raman microscope with an excitation wavelength of 785 nm over the range 325-1500 cm^{-1}. The exposure time and laser power were adjusted to maximize the signal-to-noise level while preventing sample damage. Spectral mapping was accomplished using Renishaw's software in StreamLine Map mode. The spatial resolution under the measuring conditions was approximately 1.9 μm/pixel.

6.3.4 Scanning Electron Microscopy (SEM) and Optical Microscopy

Scanning electron microscopy was conducted using a Tescan Mira3. Imaging was conducted at 10 kV acceleration voltage. Unpolymerized fiber-welded samples were gold sputtered prior to analysis to prevent sample charging. Polyionic biocomposites did not undergo gold sputtering prior to SEM characterization due to their ability to adequately conduct electrons during imaging. High resolution optical images were obtained using a Zeiss Axio Imager at 100x magnification. No sample preparation was required prior to analysis.

6.3.5 Thermogravimetric Analysis (TGA)

Themogravimetric analysis (TA Q500) was used to evaluate the thermal stability of MVIMPhos in air and in N_2. Samples were evaluated under conditions similar to the isothermal welding experiment (60°C for 60 min) and subsequent thermal initiation polymerization experiment (80°C, 90°C or 100°C for 120 min) as discussed in this report. Analysis of the TGA data was conducted using TA Universal Analysis software.

6.3.6 Density-Functional Theory (DFT)

DFT calculations were conducted by Dr. Jeremiah Woodcock at the National Institute of Standards and Technology using B3LYP functional hybrid theory with a 6311+G(2df,2p) basis set to obtain equilibrium geometries and ground state and energies. Orbital volumes were visualized using Spartan '18. This computational methodology was used to approximate the relative orbital volumes for the Poly-ILs and Poly-IL radicals with their respective counter ions to screen for possible steric hindrance.

7. Results and Discussion

The four most promising Poly-ILs were extensively evaluated: EVISCN, EVITFAc, EVIEPhos, and MVIMPhos (Figure 6). These Poly-ILs were first evaluated for their ability to weld cotton yarn substrates and polymerize ex-situ (Table 1). When both initial tests were successful, additional experiments were conducted to synthesize polyionic biocomposites.

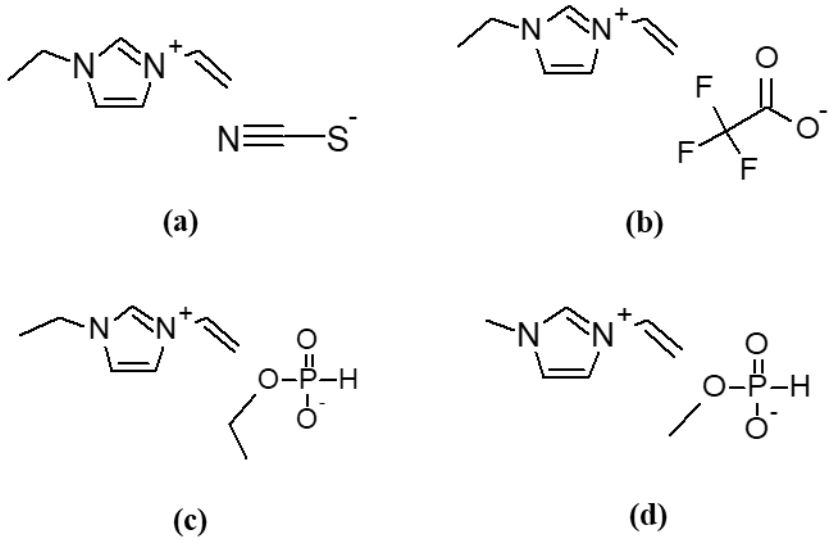

Figure 6. Poly-ILs investigated in this study, (a) 1-ethyl-3-vinylimidazolium thiocyanate, (b) 1-ethyl-3-vinylimidazolium trifluoroacetate, (c) 1-ethyl-3-vinylimidazolium ethylphosphonate, (d) 1-methyl-3-vinylimidazolium methylphosphonate

Table 1. Summary of Poly-IL Evaluations

Ionic Liquid Name	Welding Tests	Polymerization Tests
EVISCN	Unsuccessful	Successful, hard plastic
EVITFAc with BHT	Unsuccessful	Successful, thin film
EVIEPhos	Successful	Successful, soft plastic with neat Poly-IL or hard plastic with 3 wt% MCC
MVIMPhos	Successful	Successful, hard plastic

7.1 Synthesis of Novel Poly-ILs

The ^{1}H NMR spectra (Figures A-1, A-2, A-6, and A-7) show that EVISCN, EVITFAc, EVIEPhos, and MVIMPhos were successfully synthesized. However, discoloration in the EVISCN and EVITFAc solutions indicated the presence of a contaminant or degradation product. An initial sample of EVISCN had a melting point of approximately 60 °C and was light amber in color. When EVISCN synthesis was attempted a second time, the resulting EVISCN was a thick, dark-amber liquid at room temperature. Further evidence of contamination was indicated during

the anion exchange process when the column eluent was opaque instead of clear. One possible source of contamination is the anion exchange resin, which had developed a white precipitate in the beads after multiple regenerations.

Discoloration was also observed during the alkylation reaction of 1-vinylimidazole and alkyl halides. The BVICl and HVICl solutions initially phase-separated from the reactants as clear colorless solutions. However, after approximately two weeks of reacting, the Poly-IL phases acquired an amber color. While discoloration does not impact the welding capability of the Poly-ILs, UV-Vis and ex-situ polymerization experiments suggest it may affect HMPP's ability to initiate polymerization by absorbing photons in the wavelength of initiation (ca. 250 nm).

An initial synthesis of Poly-ILs with a trifluoroacetate anion had undergone uncontrolled autopolymerization prior to the addition of an initiator and irradiation with UV light. Autopolymerization of the Poly-IL inhibits welding experiments and further polymerization with HMPP. Therefore, to ensure successful synthesis of the Poly-IL monomers and control of the polymerization process, EVITFAc and BVITFAc were prepared with 1 mole% BHT, a free-radical inhibitor. Addition of the BHT enabled the synthesis of the EVITFAc and BVITFAc Poly-ILs without significant autopolymerization. In order to overcome the BHT inhibitor, slightly higher concentrations of photoinitiator were required to polymerize the EVITFAc. Futures tests with BVITFAc are being planned.

To minimize contamination and possible water up-take during synthesis, metathesis reactions were conducted to synthesize Poly-ILs with trifluoroacetate and benzoate anions. The synthesis of BVITFAc with BHT was conducted via metathesis and resulted in a clear amber room-temperature liquid Poly-IL that did not autopolymerize. NMR and ATR-IR of the BVITFAc (after filtration of the ammonium chloride) indicated that the reaction was successful, but did not run to completion (Figure A-5). Future steps to remove excess reactants from metathesis products include vacuum drying the filtrate. Additionally, allowing the reaction to continue for longer times or at increased temperatures may further the extent of the reaction.

7.2. Evaluation of Poly-ILs

7.2.1 EVISCN

EVISCN was investigated based on the findings of Swatloski *et al.*, who reported ILs with thiocyanate anions had successfully dissolved pulp cellulose upon treatment with microwave heating.[7] EVISCN experiments sought to expand upon these findings to combine the thiocyanate anion with a 1-ethyl-3-vinylimidazolium cation, which had previously demonstrated the ability to polymerize and weld cellulose when paired with a halide anion.[26]

7.2.1.1 Polymerization of EVISCN

Polymerization experiments of EVISCN:1 mole% HMPP solutions formed hard plastics which demonstrated hygroscopic properties, similar to those observed by Chung *et al.*,[26] upon exposure to the atmosphere. Attempts to reproduce these experiments with a second batch of EVISCN produced thin films that melted into viscous solutions of partial polymerized material when heated (Figure 7). The lack of reproducibility is likely caused by contaminants within the second batch of EVISCN (due to anion exchange column contamination).

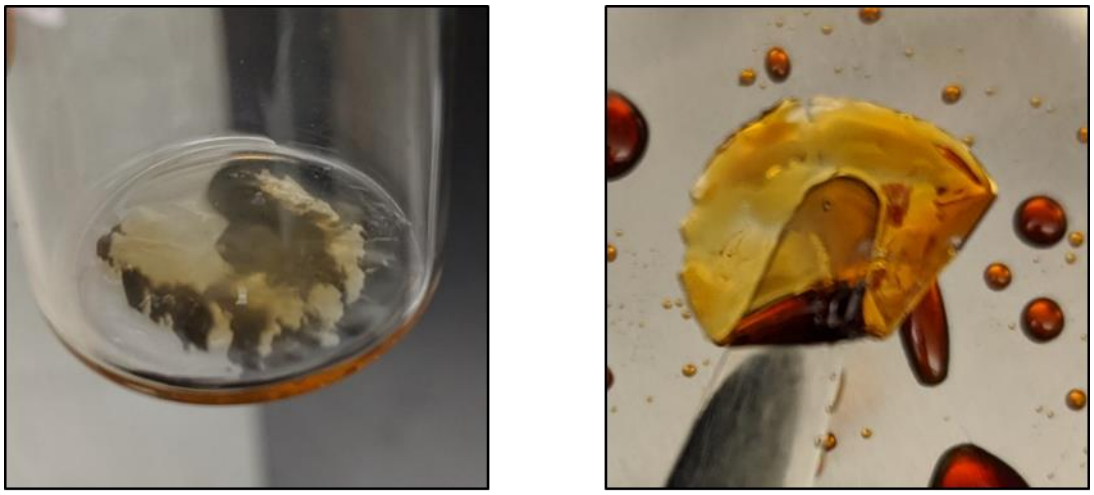

(a) (b)

Figure 7. Optical images of (a) EVISCN polymerized into a hard plastic, and (b) EVISCN polymerized into a thin film.

7.2.1.2 NFW Experiments with EVISCN

EVISCN was initially evaluated as a NFW solvent by dissolving 1 wt% MCC using heat and stirring. Some MCC sample appeared to dissolve into solution at 100 °C, which suggested EVISCN had good potential biopolymer solvent properties. However, welding experiments conducted with cotton yarn substrates at 60 °C did not result in a welded product. Further welding experiments were investigated following the procedure outlined by Swatloski *et al.*,[7] using a microwave heating source. Multiple power settings and exposure times were implemented in an effort to determine adequate parameters to enable successful welding (Table 2). Characterization of the treated cotton yarns was conducted using SEM (Figure 8) or an optical microscope.

Table 2. Results from EVISCN microwave welding experiments. *Samples were not heated continuously.

Microwave Welding Experiments		
Power (W)	Time (min)	Result
140	10*	No Welding
200	3	No Welding
252	1.5 and 3*	No Welding
300	1	Yarn Substantially Degraded

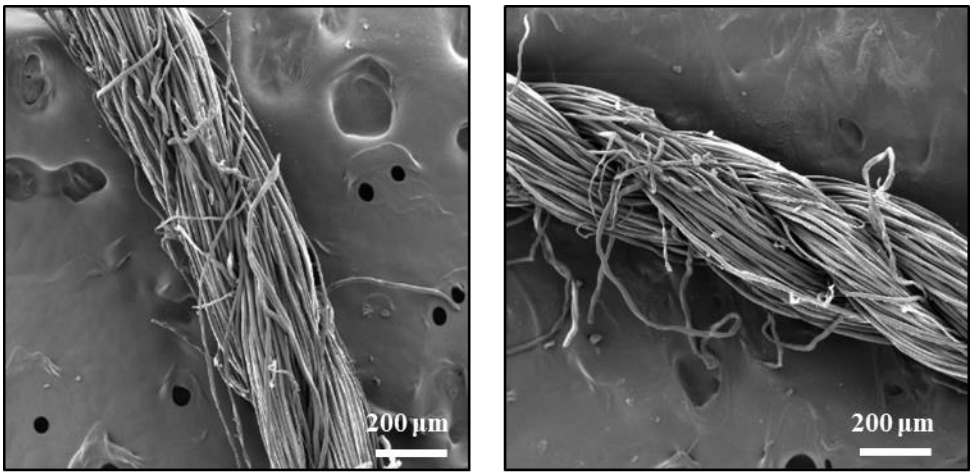

Figure 8. Scanning electron microscopy of (a) untreated cotton yarn, and (b) cotton yarn treated with EVISCN by microwave (140 W for 10 min).

Figure 8a is a control sample of a cotton yarn before being treated with EVISCN. The image displays a multitude of cotton fibers on the yarn's surface that lack consolidation. Figure 8b does not demonstrate any noticeable differences from the untreated yarn. A successfully fiber-welded yarn would have considerable consolidation of material and a "webbing" of reconstituted cellulose material on the surface.[11] After observing that welding did not occurred, the microwave welding parameters were increased, exposing the yarns and EVISCN to higher temperatures and longer welding times. Higher power microwave experiments produced results similar to the 140W treatment.

Exposing the EVISCN and cotton yarn to 300W for 1 min severely degraded the cotton substrate and the Poly-IL. The resulting solution was dark amber in color, had a burnt scent, and appeared to have a substantially higher viscosity. Attempts to reconstitute cellulose from this EVISCN solution with a water rinse failed, suggesting that the cellulose microstructure within the cotton yarn had degraded. Polymerization experiments with post-treatment EVISCN also failed, indicating an appreciable amount of degradation occurred to the vinyl functional group. Due to these results, no further experiments were conducted using EVISCN.

7.2.2 EVITFAc

Previous work by Chung *et al.*,[26] attempted to polymerize 1-ethyl-3-vinylimidazolium acetate, but were unsuccessful. The DFT data suggested that EVI Acetate (Figure A-8) experienced significant steric hindrance of the radical species during polymerization, and that a Poly-IL consisting of a 1-ethyl-3-vinylimidazolium cation and a trifluoroacetate anion would have less crowding (Figure A-9). Therefore, EVITFAc was synthesized and evaluated for its ability to polymerize and be used as an NFW solvent.

7.2.2.1 Polymerization of EVITFAc with BHT

Polymerization experiments of EVITFAc with BHT were conducted with various concentrations (i.e., 1 mole%, 2 mole%, and 6 mole%) of HMPP photoinitiator. Each solution demonstrated low degrees of polymerization, resulting in thin films of polymerized material (Figure 9). These results were similar to the experiments conducted with contaminated EVISCN. The EVITFAc thin films also demonstrated hygroscopic properties and melted when heated. One possible explanation for this result is that these EVITFAc solutions began to crystallize as the temperature dropped below the approximate melting point of EVITFAc (ca. 90 °C) when the 120V/100W mercury vapor lamp was turned off.

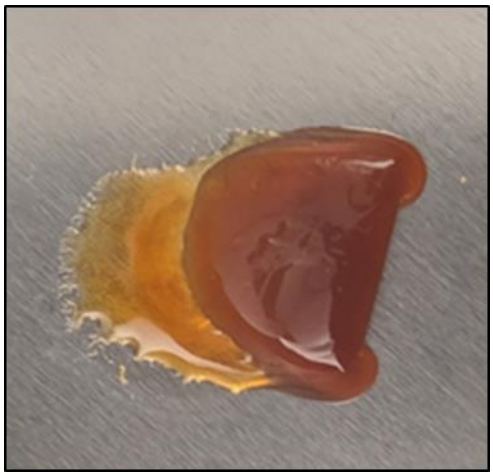

Figure 9. Optical image of polymerized EVITFAc

The presence of contaminants in the EVITFAc is another potential cause for the low degree or lack of polymerization. The HMPP photoinitiator initiates radical chain growth polymerization by absorbing light in the 250 nm region and forming radical species. However, absorbance of photons in the 250 nm region by contaminants in the Poly-IL solution would inhibit the HMPP photoinitiator. To determine the absorbance region of the EVITFAc solutions, UV-Vis spectroscopy experiments were conducted with neat EVITFAc in pathlengths of 1 mm and 10 mm (Figure 10).

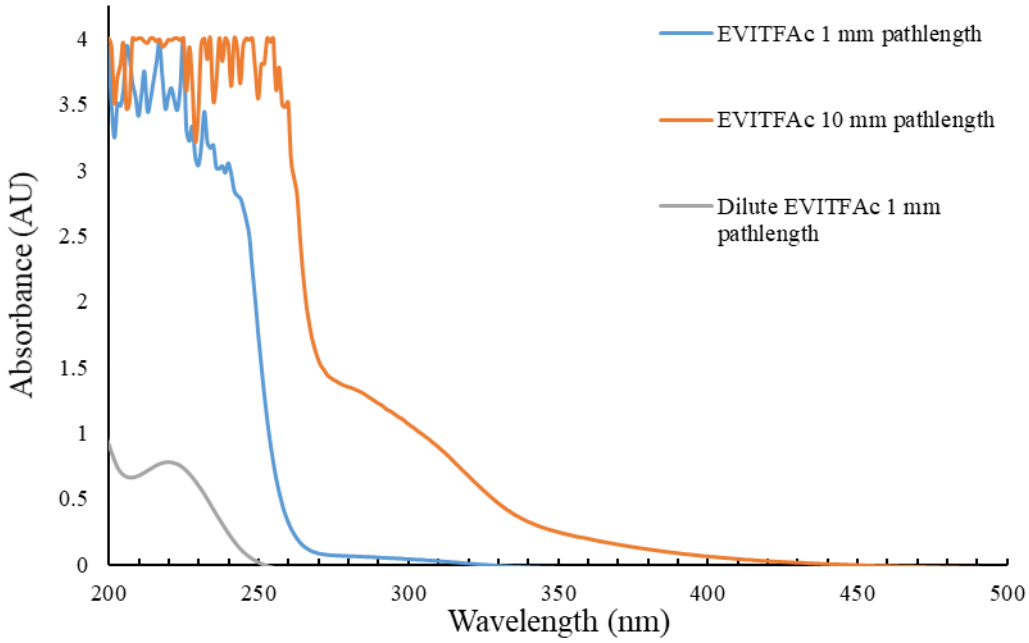

Figure 10. UV-Vis results of EVITFAc samples with 1 mm and 10 mm path length

Large absorbance values between the 200 and 260 nm region in the samples with minimal dilution indicates absorbance in the same region as the photoinitiator, which likely limited the degree of polymerization. However, the presence of solid thin films on the surface of samples in these experiments does suggest that some polymerization did occur, although it did not extend throughout the bulk of the material.

Polymerization was confirmed via ^{1}H NMR characterization of a polymerized EVITFAc:6 mole% HMPP sample that had been dissolved in DMSO-d_6. The resulting spectrum (Figure A-10) contained multiple small peaks adjacent to the peaks found in the ^{1}H-NMR of neat EVITFAc with BHT (Figure A-2). These additional peaks are present due to the splitting of the imidazolium ring protons by neighboring imidazolium rings in the polymer chain. However, the lack of multiple broad peaks, like those previously observed by Chung *et al.*,[11] indicate a lower degree of polymerization than previously obtained with Poly-ILs in our laboratory. A new batch of EVITFAc has recently been prepared, via a metathesis, and appears to be less contaminated. Future experiments are planned with this less contaminated batch of EVITFAc, and will hopefully demonstrate improved polymerization capabilities.

7.2.2.2 NFW Experiments with EVITFAc

Initial MCC dissolution experiments with EVITFAc were characterized with ATR-IR spectroscopy. The ATR-IR spectra (Figure 11) of neat EVITFAc and the reconstituted precipitate from an EVITFAc:3 wt% MCC solution indicate O-H stretches (ca. 3300 cm^{-1}) and C-O stretches (ca. 1050 cm^{-1}). These results suggest that MCC was successfully recovered from the EVITFAc solution and that EVITFAc has potential as an NFW solvent.

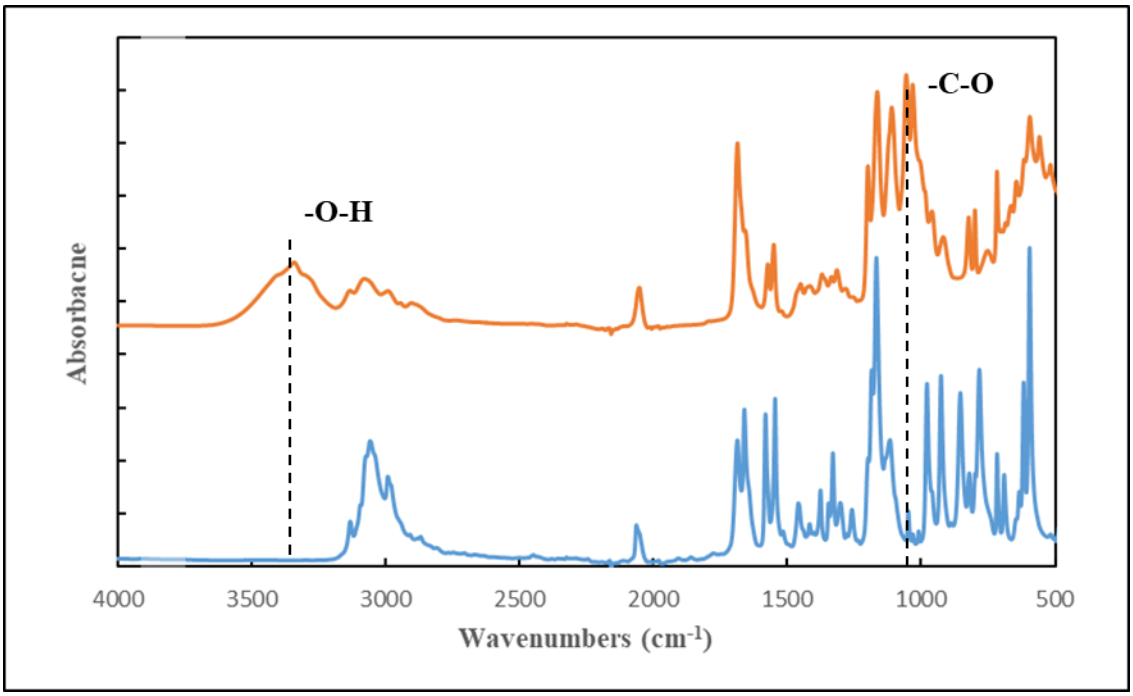

Figure 11. ATR-IR spectra of neat EVITFAc (blue) and reconstituted MCC from 3 wt% MCC:EVITFAc (orange)

NFW experiments were conducted by treating cotton yarns in a N_2 atmosphere glovebox at 60 °C for 100 min. An ACN co-solvent was used to decrease the viscosity of the EVITFAc. Higher viscosities inhibited the Poly-IL from adequately wetting the yarn and initiating welding. The optical images of the EVITFAc-treated cotton yarn in Figure 12 show no significant differences, indicating that welding was unsuccessful (compare Fig 12a to 12b).

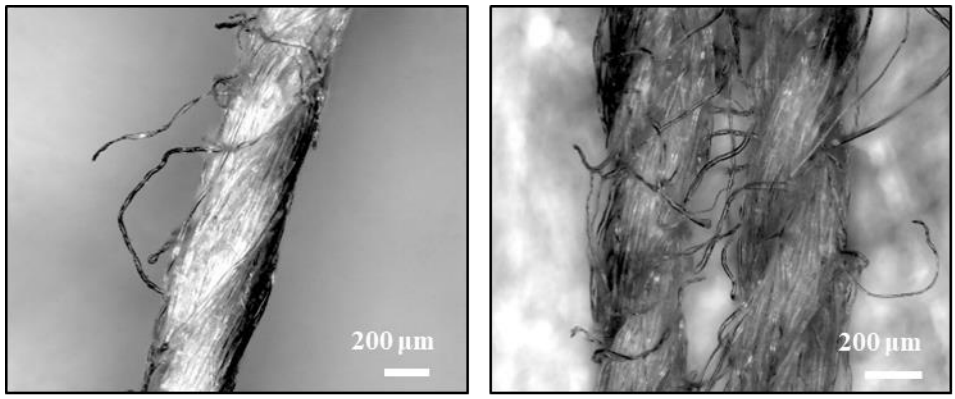

Figure 12. Optical images of, (a) untreated cotton yarn and (b) cotton yarns treated with EVITFAc (100 min, 60 °C).

The lack of welding is attributed to the low (60 °C) temperature at which the EVITFAc NFW experiments were conducted. The observed melting point of neat EVITFAc was approximately 80°C, and the Poly-IL became substantially less viscous at 90°C. In retrospect, it is likely that the ACN evaporated at 60 °C, leaving behind the neat EVITFAc to resolidify during the welding process. EVITFAc solidification would likely limit the ability for the EVITFAc to penetrate the biopolymer and weld the matrix. Future experiments at elevated temperatures may demonstrate the potential for neat EVITFAc (and BVITFAc) to act as successful NFW solvents.

7.2.3 EVIEPhos

Experiments with EVIEPhos (and MVIMPhos) were motivated from the results of several reports that demonstrated the ability for alkylphosphonate-based ILs to dissolve cellulose.[27-29]

7.2.3.1 Polymerization of EVIEPhos

Successful, reproducible polymerization was achieved with EVIEPhos. Solutions of EVIEPhos:3 wt% MCC with HMPP (1 mole% with respect to the EVIEPhos) produced hard plastics when irradiated for 1 hr with the 120V/100W mercury vapor lamp. The polymerized material had minimal deformation when exposed to pressure, but still demonstrated hygroscopic properties when exposed to the atmosphere outside of the glovebox. Solutions of EVIEPhos:2 mole% HMPP demonstrated a lower degree of polymerization than solutions with MCC, forming a viscous liquid instead of a hard plastic. This may be the result of the MCC acting as a binder within the new polymer matrix, thereby producing harder materials. EVIEPhos experiments also indicated that the degree of polymerization was influenced by the time of exposure to the UV source. Neither EVIEPhos solution demonstrated appreciable degrees of polymerization after 3 min of irradiation; however, when irradiated for 1 hr both samples exhibited phase changes to a solid material.

7.2.3.2 NFW Experiments with EVIEPhos

Experiments conducted with EVIEPhos successfully produced welded substrates. Cotton yarns were treated with EVIEPhos at 90°C for 60 min in the N_2 atmosphere glovebox. After 60 min the yarns appeared swollen, indicating the EVIEPhos had sufficiently wetted the material. Additional swelling in areas not originally wetted with the Poly-IL indicates that the EVIEPhos had a low enough viscosity to wick along the yarns. Following quenching and reconstitution, the structure and morphology of the EVIEPhos-treated yarns were characterized with SEM (Figure 13).

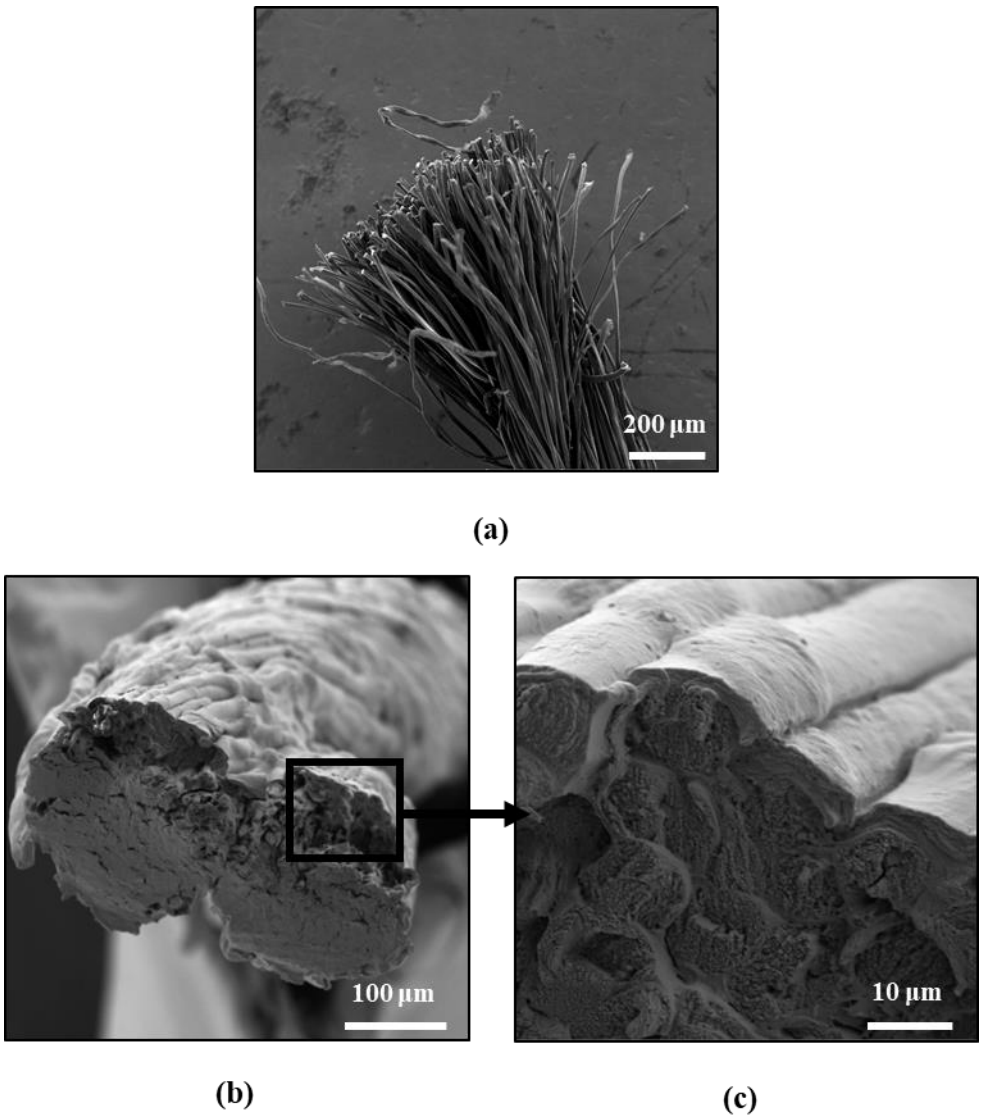

Figure 13. Scanning electron microscopy images of, (a) untreated cotton yarn, (b) low resolution and, (c) higher resolution images of cotton yarn fiber-welded with EVIEPhos.

The region at the top of Figure 13b illustrates the surface of the treated yarns. Individual fibers have consolidated on the surface of the yarns and there appears to be a coating of biopolymer material that conjoins the fibers. Further, the image depicts the region between the two yarns where the mobilized material had propagated and been reconstituted in a manner that welds the yarns together. Figure 13c shows the depth at which the EVIEPhos and mobilized material penetrated the yarn matrix. While the structure of the fibers has been altered, there are clear veins of material that extend down from the surface and in-between the fibers located within the yarn. Additionally, the consolidated material on the surface is readily apparent, coating the exterior of individual fibers and linking adjacent fibers together. These images demonstrate the ability for EVIEPhos to adequately weld the surface of the cotton yarn substrates and permeate into the

biopolymer matrix. These results, combined with the successful polymerization, make EVIEPhos a promising candidate for creating polyionic biocomposites.

7.2.3.3 Synthesis of Polyionic Biocomposites with EVIEPhos

Novel polyionic biocomposites were successfully prepared from cotton yarns and EVIEPhos. A solution of EVIEPhos:1 mol % HMPP photoinitiator was prepared and heated to 90 °C for 5 min to lower the viscosity of the solution. The EVIEPhos:HMPP solution was then applied to cotton yarns in parallel and perpendicular configurations for 60 min at 90 °C. After 60 min the treated yarns appeared swollen from the uptake of the Poly-IL solution. Observations also indicated the successful mobilization of the material as the two parallel yarns were now indistinguishable and appeared to form one yarn. Following polymerization of the EVIEPhos by irradiating the samples with a UV light for 30 min, the yarns appeared to consolidate further and decrease in diameter. These physical changes mirrored the observations of standard NFW experiments and were the first indications of a successful welding and polymerization sequence to form a polyionic biocomposite. The biocomposite's surface and cross-section were characterized using SEM (Figure 14).

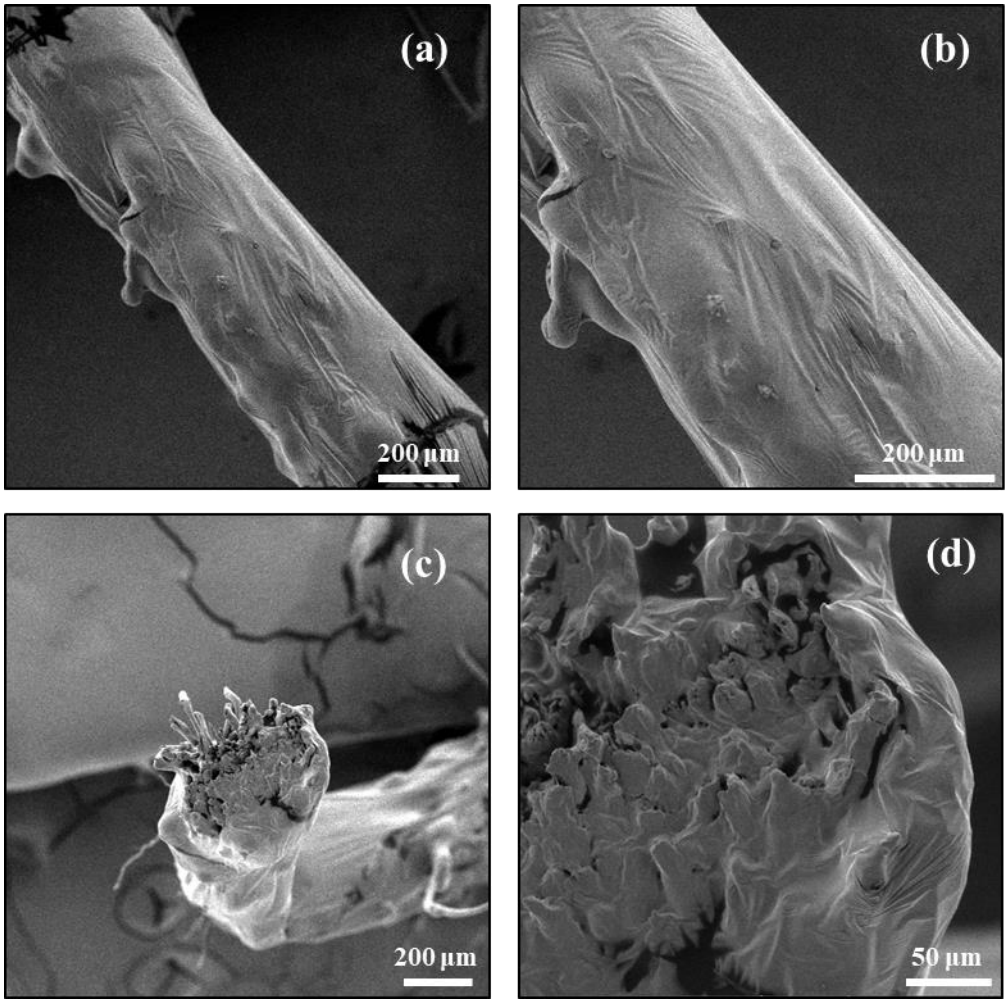

Figure 14. Scanning electron microscopy of a polyionic biocomposite synthesized with EVIEPhos showing (a) low-resolution surface image, (b) high-resolution surface image, (c) low-resolution cross-section image, (d) high-resolution cross-section image.

Figure 14a and 14b indicate a relatively smooth surface with small wrinkles scattered across the yarn. This surface feature resembles the shell of mobilized cotton present in substrates that have undergone extensive welding. However, this degree of welding is not present in the cotton substrates welded at the same temperature and time (see Figure 13). Comparison of these figures suggests that the surface features are the result of an EVIEPhos polymer coating on the surface of the welded yarn. The polymer coating appears more readily in Figure 14d, in which the edge of the cotton yarn is encompassed by the amorphous coating. These observations are unique to the EVIEPhos polyionic biocomposite. In Figure 13c, which illustrates welding quenched with the removal of EVIEPhos, the individual fibers are distinguishable on the surface of the yarn and around the edges of the cross section. This suggests that the surface features in Figure 14 are the result of the polymerization of the EVIEPhos on the surface of the welded yarn.

7.2.4 MVIMPhos

While EVIEPhos demonstrated the ability synthesize polyionic biocomposites, experiments soon shifted to MVIMPhos due to our ability to produce MVIMPhos in larger quantities with additional purification steps in accordance with the literature.[27]

7.2.4.1 Polymerization of MVIMPhos

Polymerization of MVIMPhos was conducted via photo- and thermal-initiation using HMPP and potassium persulfate initiators, respectively. Solutions of MVIMPhos:1 mole% HMPP were initiated with a 120V/100W mercury vapor lamp for 30 min to produce a hard plastic. Following irradiation and cooling, the poly-MVIMPhos was characterized using ^{1}H NMR, Raman, and ATR-IR spectra (Figures 15 - 18).

Comparison of the ^{1}H NMR spectra of neat MVIMPhos (Figure 15) and polymerized MVIMPhos (Figure 16) indicated successful polymerization. The polymerized MVIMPhos spectra exhibits an additional alkane peak that is not present in the neat MVIMPhos spectrum. This peak corresponds to the new bonds formed between imidazolium rings during the polymerization process. Further, additional small peaks are discernable in the polymerized MVIMPhos spectrum which can be attributed to the increased splitting caused by the protons on adjacent imidazolium rings.

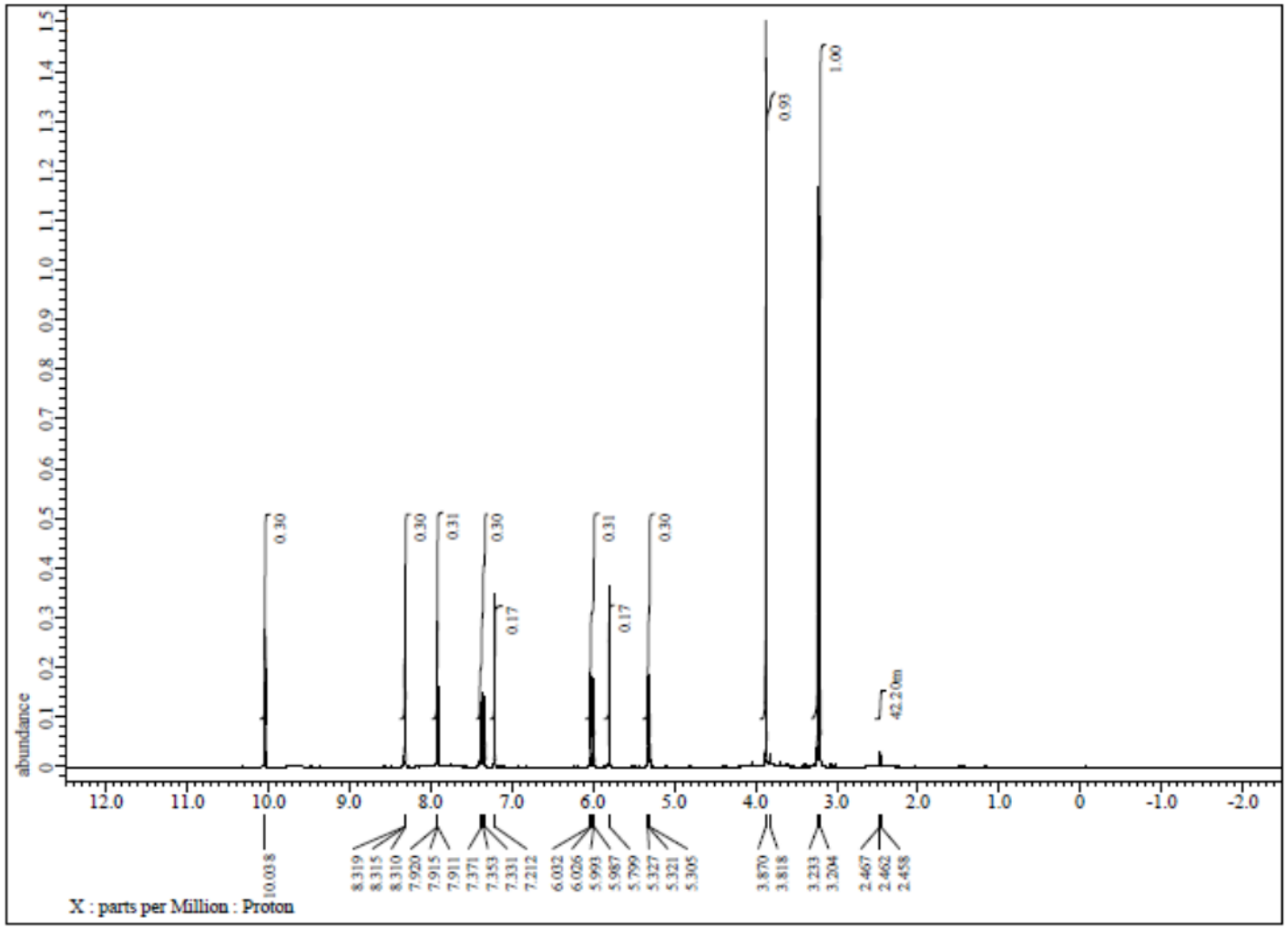

Figure 15 ^{1}H NMR spectrum of neat 1-methyl-3-vinylimidazolium methylphosphonate

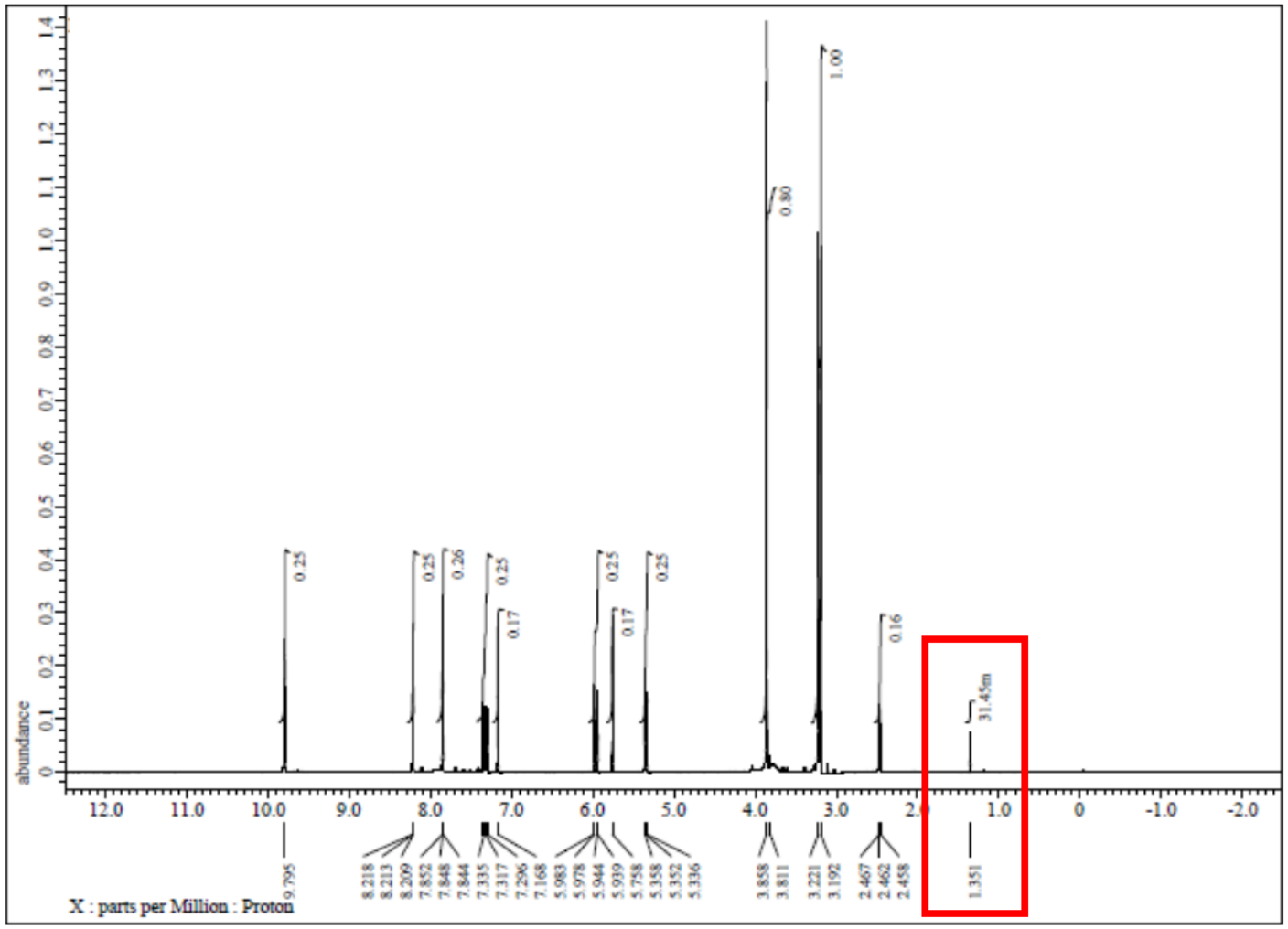

Figure 16 [1]H NMR spectrum of polymerized 1-methyl-3-vinylimidazolium methylphosphonate with red inset indicating the presence of a new peak in the alkane (C-C) region of the spectra

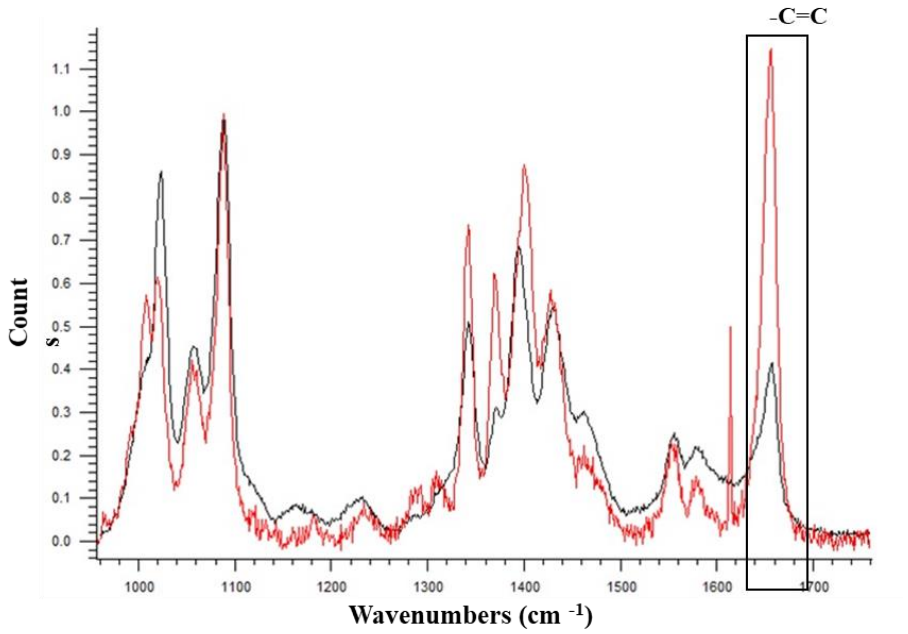

Figure 17. Raman spectra of 1 mole% HMPP:MVIMPhos preinitiation (red) and after UV irradiation for 30 min (black).

Analysis of the sharp C=C peak (ca. 1660 cm^{-1}) in the Raman spectrum indicates the relative concentration of the vinyl group present in the MVIMPhos monomer. Comparison of the normalized Raman spectra demonstrates a substantial decrease in the concentration of the vinyl group after initiation. While a sufficient signal was acquired, numerous challenges were encountered to produce adequate results. Polymerized MVIMPhos samples frequently exhibited extensive fluorescence that overwhelmed the resulting Raman spectra. A sufficient signal was acquired by focusing on a very small sample of MVIMPhos and bleaching the sample for 30 seconds before taking the measurement.

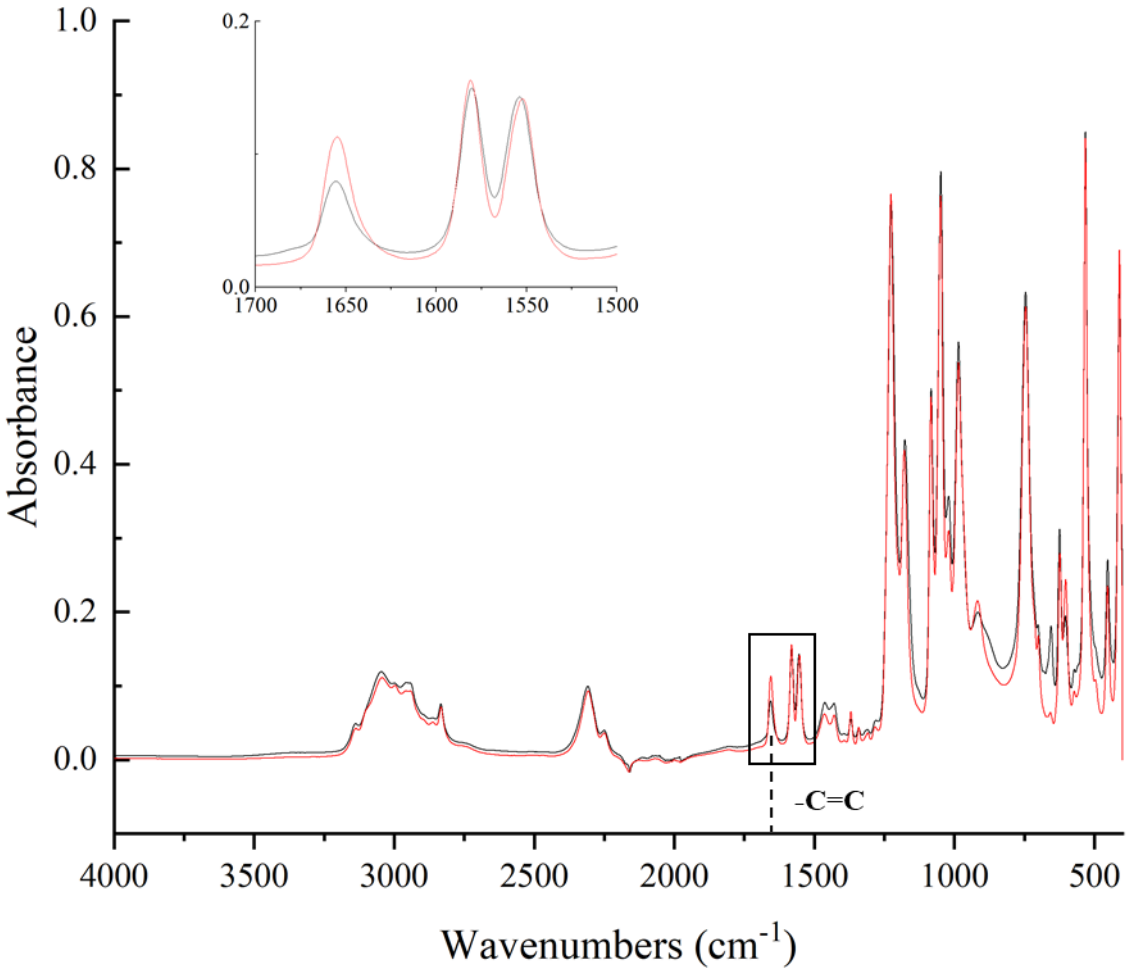

Figure 18. ATR-IR spectra of neat MVIMPhos (red) and poly-MVImMPhos (black) from 1 mole% HMPP:MVIMPhos after UV irradiation for 30 min.

Results from the Raman spectra were supported by analysis of the C=C stretch (ca. 1655 cm^{-1}) in the ATR-IR spectra Comparison of the neat and polymerized MVIMPhos spectra indicate a decrease in the concentration of the vinyl group after polymerization. This decrease, along with the change in physical properties supports successful polymerization. However, the continued presence of the peak post-initiation also indicates the presence of residual MVIMPhos monomer. Further experiments altering the concentration of the initiator or extending irradiation time may discover conditions that result in a greater extent of polymerization when using photoinitiators.

Polymerization via thermal initiation was conducted using solutions of MVIMPhos:1 mole% potassium persulfate. The potassium persulfate initiator was chosen because it is an ionic compound that is soluble in the MVIMPhos. Solutions of MVIMPhos containing persulfate became substantially more viscous over a period of 24 hr, indicating polymerization could occur slowly at room temperature. The effect of temperature and time on the extent of polymerization was evaluated by polymerizing samples of MVIMPhos:1 mole% potassium persulfate solutions at

60 °C, 80 °C, and 100 °C for times ranging from 5 to 45 min. The resulting polymers were characterized using ATR-IR spectroscopy (Figure 19).

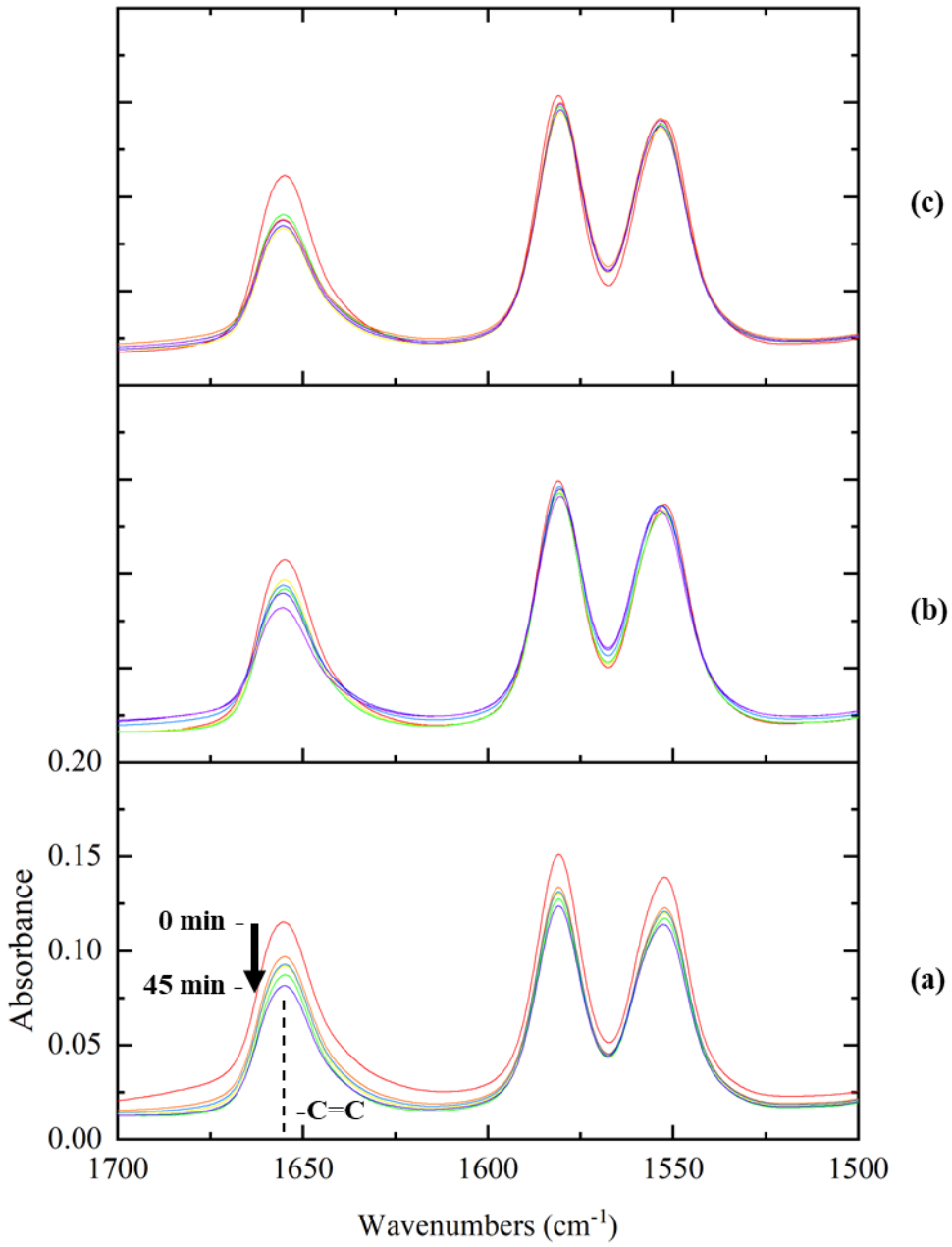

Figure 19. ATR-IR spectra of MVIMPhos samples polymerized at (a) 60 °C, (b) 80 °C, and (c) 100 °C for times ranging from 0 min to 45 min (as indicated by the arrow in frame (a)). A similar reduction in the C=C stretch was observed in the spectra at each welding temperature. Spectra were peak normalized to the stretch at ca. 2830 cm^{-1} which is present in each sample with invariant intensity.

Similar to the analysis of Figure 18, the C=C stretching peak (ca. 1655 cm^{-1}) was used to determine the relative extent of polymerization. Each spectrum demonstrates a decrease in vinyl group concentration with an increase in polymerization time. Additionally, all of the ATR-IR spectra indicate the presence of residual MVIMPhos monomer, as the vinyl peak persists even after being exposed to 100 °C for 45 min. The continued presence of the vinyl peak suggests a significant concentration of monomer remains after polymerization. Further, while the vinyl peak generally decreases with increase polymerization time, there appears to be a time at which the concentration change of the vinyl functional group is minimal. This result suggests that there is a time beyond which polymerization proceeds at a slower rate.

7.2.4.2 NFW Experiments with MVIMPhos

Successful welding was also achieved when cotton yarns were treated with MVIMPhos. Cotton yarns were treated with MVIMPhos at 92 °C for times ranging from 10 min to 30 min. After quenching and reconstituting with rinses of methanol and water, the treated yarns were potted in epoxy and cross sectioned. Characterization of the cross-sections using Raman spectroscopy produced spectral contour plots for each sample (Figure 20). The contour plots measure the relative intensity of a peak at 380 cm^{-1}, which decreases as the extent of welding increases, compared to a peak at 354 cm^{-1}, which remains unchanged during the welding process.

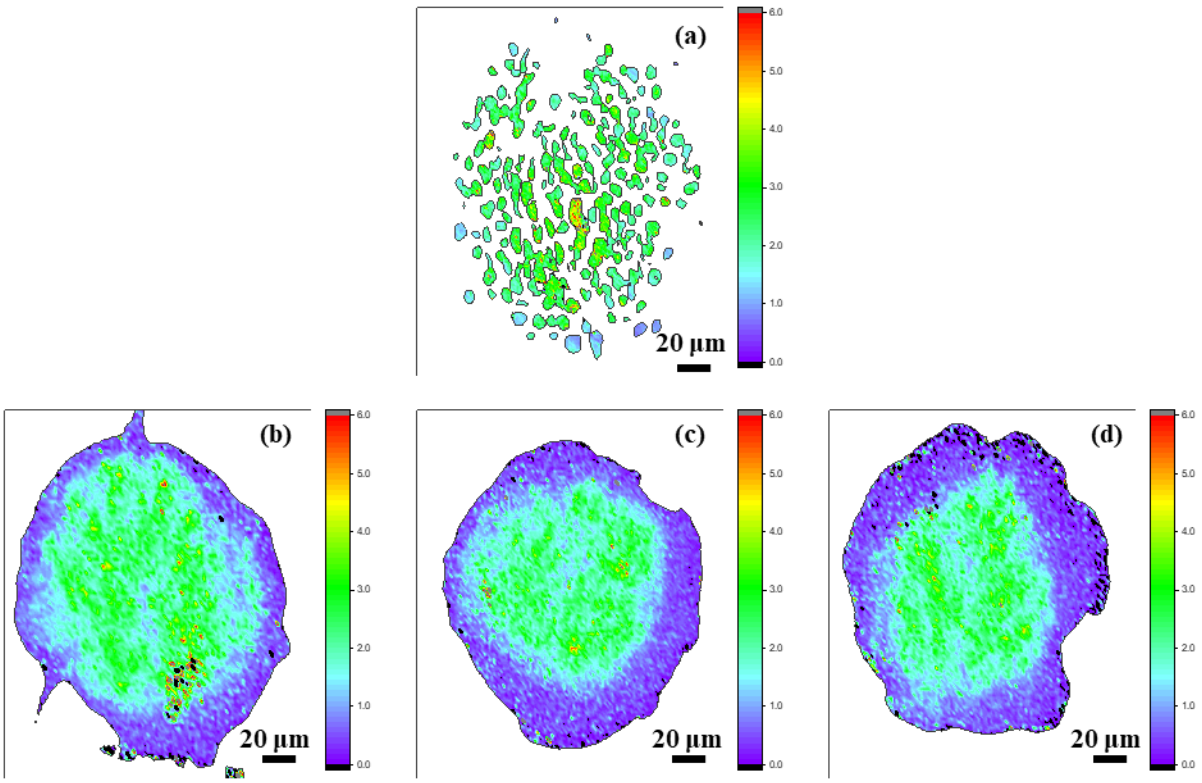

Figure 20. Cross-section contour plot of the intensity ratio between 380 cm^{-1} and 354 cm^{-1} peaks for cotton yarns welded with MVIMPhos at 92 °C at various times, (a) 0 min treatment (untreated control), (b) 10 min treatment time, (c) 20 min treatment time, and (d) 30 min treatment time.

One of the most noticeable features is the ability to distinguish individual fibers in the untreated cotton yarn (Fig 20a). Once the yarn has been treated with MVIMPhos, it undergoes considerable consolidation as seen in the Figures 20b, 20c, and 20d, similar to what was observed in SEM images of cotton welded with EVIEPhos (see Figure 13). Present in each frame of the treated yarns is a 'violet ring' on the outermost edge of the yarn that increases with welding time. This violet ring represents the outer regions of the yarn that have undergone a transition from crystalline (the light-green colored core) to amorphous cellulose, as a result of biopolymer interactions with the MVIMPhos during fiber-welding. This effect clearly increases with welding time, as shown in Fig 20b-d. These contour plots support the successful welding of cotton substrates and demonstrated the potential for MVIMPhos to synthesize polyionic biocomposites.

7.2.4.3 Synthesis of Polyionic Biocomposites with MVIMPhos

Following the successful polymerization and welding experiments, MVIMPhos was used to synthesize polyionic biocomposites. These experiments were conducted using the potassium persulfate thermal initiator. A thermal initiator was chosen in an effort to produce a more thorough and consistent polymerization throughout the biocomposite matrix, as previous experiments with photoinitiators had only achieved polymerization on the surface of the welded substrate.

Polyionic biocomposites were synthesized by treating cotton yarns with a solution of MVIMPhos:1 mole% potassium persulfate for times ranging from 5 min to 60 min at 60 °C. The temperature was then increased to 100 °C for 19 hr to initiate polymerization. A lower welding temperature was selected to minimize the extent of polymerization occurring during the welding process. Extensive polymerization times were utilized to ensure sufficient polymerization of the material. After polymerization, the polyionic biocomposites were characterized using SEM (Figure 21). Due to the ability of the polymerized MVIMPhos to conduct electrons, a gold sputter coating was not required to obtain the SEM images.

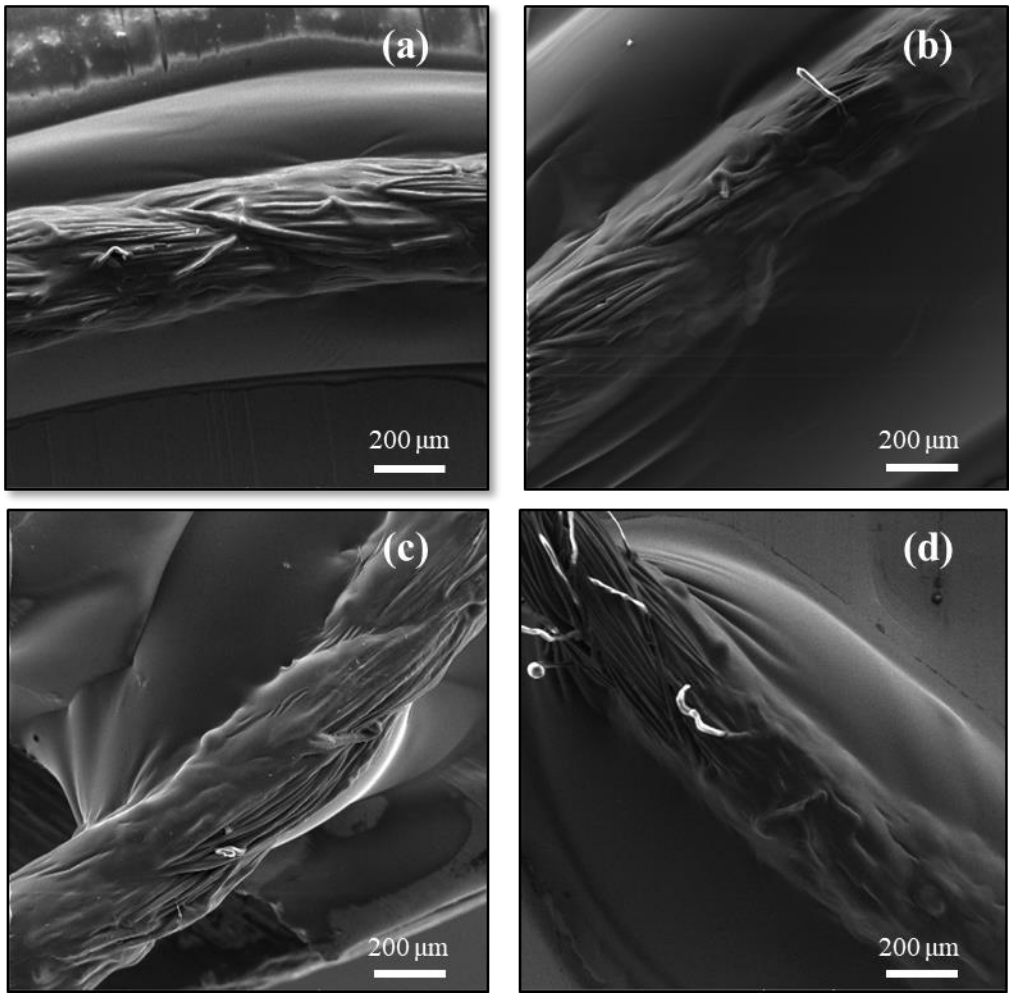

Figure 21. Scanning electron microscopy of polyionic biocomposites produced via welding with MVIMPhos:1 mole% potassium persulfate solution at 60 °C for (a) 5 min, (b) 15 min, (c) 45 min, and (d) 60 min. After welding, each sample was polymerized at 100 °C for 19 hr.

Each of the images in Figure 21 demonstrates material consolidation, as many of the fibers have coalesced into one welded bundle. This observation indicates that the welding step of the synthesis process was successful. In addition, a coating of polymerized MVIMPhos appears to cover each of the welded yarns, which suggests the polymerization step was also successful. The ability for the polymerized MVIMPhos to conduct electrons is demonstrated in Figure 21d. In this figure there are a few fibers protruding from the yarn that appear bright white in color. This coloration is caused by the buildup of charge on the non-conductive yarns, which is the standard appearance of cotton yarns that have not been sputter-coated before SEM analysis. However, the buildup of charge is not present along the remainder of the fibers that have been treated and coated with the polymerized MVIMPhos. These results support the conclusion that the resulting polyionic biocomposites are conductive.

7.2.4.4 Thermogravimetric Analysis of MVIMPhos

Due to the elevated temperatures and extended polymerization times used to synthesize the MVIMPhos-based polyionic biocomposites, TG analysis of neat MVIMPhos was conducted to investigate potential degradation of the Poly-IL (Figure 22). Samples of neat MVIMPhos were heated in an N_2 atmosphere at 60 °C for 60 min before the temperature was increased to either 80 °C, 90 °C, or 100 °C and held there for 2 hr.

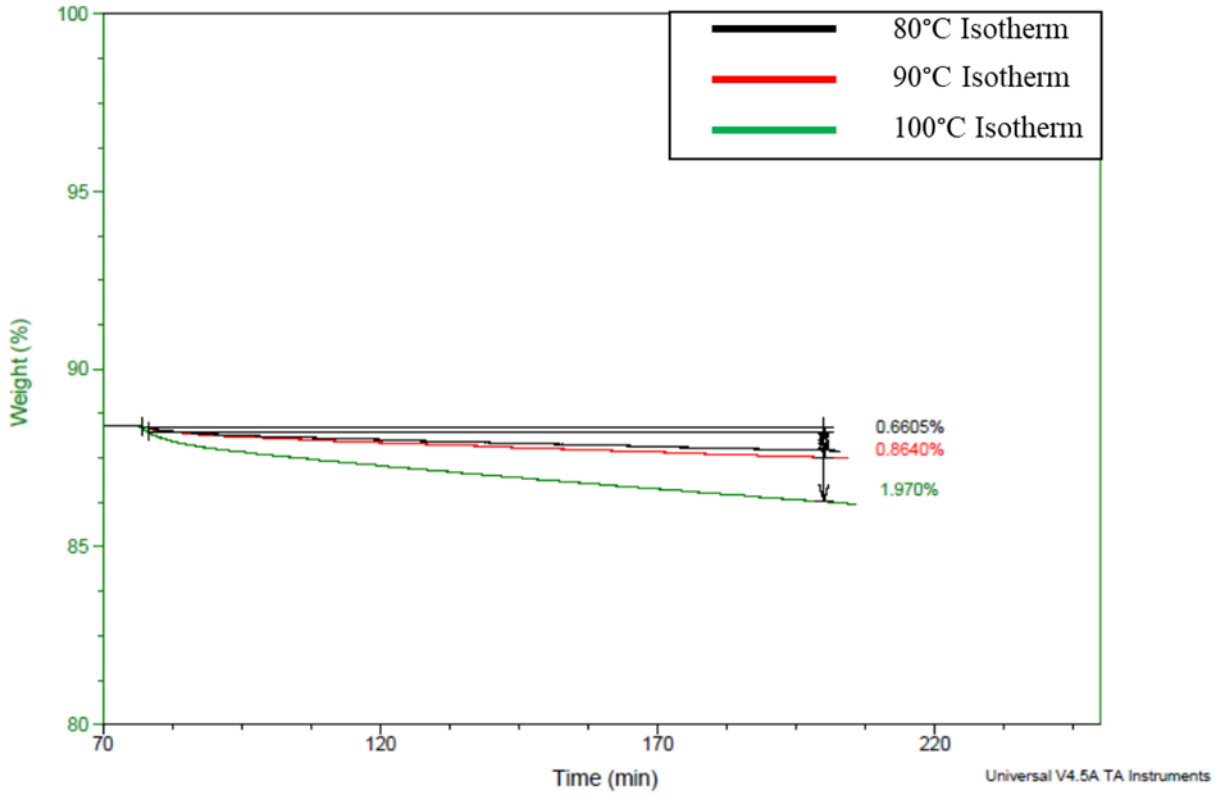

Figure 22. Thermogravimetric Analysis of MVIMPhos in N_2 at 80 °C, 90 °C, and 100 °C.

Sample weight loss was observed to occur at a constant rate once the maximum thermal temperature was reached. The onset of the weight loss was indicated by the presence of a local maximum in the first derivative of the sample weight change (ca. 77 min). In an effort to determine whether the weight changes were more substantial than the evaporation of water from the sample, a comparison was conducted between the ratio of the rate of mass loss and ratio of the changes in the heat of vaporization of water[30] (Table 3). Analysis indicates that between 80 °C and 100 °C the change in heat of vaporization for water increases at a near constant value while the ratio of mass loss doubles between 80 °C to 90 °C and 90 °C to 100 °C. This suggests that more than just the evaporation of water contributes to sample weight loss at higher temperatures. Sample analysis was also done in air and showed higher rates of mass loss most likely due to air oxidation.

Table 3. Summary of MVIMPhos TGA Data

Isothermal Temperature (°C)	Mass loss During Polymerization Isotherm (%)	Rate of Mass Loss During Polymerization Isotherm (%/min)	Heat of Vaporization (kJ/kg)	Ratio of the Rate of Mass Loss	Ratio of the Heat of Vaporization
100	1.97	0.016	417.50 (ca. 99.6 °C)	2.3	1.1
90	0.86	0.0070	377.06		
				1.3	1.1
80	0.66	0.0053	335.10		

These TGA data suggest that lower initiation temperatures would mitigate potential sample degradation over extended polymerization times. These results will be used to inform future experiments to design polyionic biocomposites while maintaining sample integrity. Additionally, fine-tuning synthesis parameters may lead to more energy efficient and timely synthesis processes.

7.2.5 Developing a method to measure conductivity of polyionic biocomposites

Rudimentary sample cells and electrochemical impedance spectroscopy (EIS) parameters were developed to measure the conductivity of various ionic solutions. These devices were intended to be applied toward measuring conductivity differences of the polyionic biocomposites. However, due to unforeseen time constraints, conductivity measurements of the polyionic biocomposites were not completed. Future characterization of the synthesized polyionic biocomposites may be possible using the EIS procedures and initial characterization work contained in Figures A-12-A14 of the appendix.

8. Conclusion

To date, ten Poly-ILs have been synthesized using combinations of alkylation reactions, mass action ion exchange, or metathesis. Metathesis reactions, as well as the addition of BHT inhibitor in Poly-ILs with trifluoroacetate anions, have been used to synthesize Poly-ILs with greater purity. Contaminants and water content inhibit the ability for Poly-IL to polymerize and weld and therefore must be minimized. Future synthesis reactions will be conducted by our lab group at lower temperatures over a longer period of time in order to minimize degradation of reactants or the product Poly-IL.

Polymerization experiments demonstrated the ability for several Poly-ILs to polymerize ex-situ using the HMPP photoinitiator and potassium persulfate thermal initiator. Initial experiments with neat Poly-ILs and HMPP resulted in thin films due to contaminants within the Poly-IL solutions absorbing photons in the same spectral region as those absorbed by the photoinitiator. However, increasing exposure time to the 120V/100W mercury vapor lamp and/or the addition of 3 wt% MCC resulted in the successful formation of hard plastics. Experiments using potassium persulfate at various temperatures indicated polymerization of MVIMPhos. However, analysis of the resulting ATR-IR spectra also indicated the presence of MVIMPhos monomer after 1 hour initiation at 100 °C. Further experiments extending the initiation time and using co-solvents to reduce the solution viscosity will be conducted to increase the extent of polymerization.

Following successful ex-situ polymerization, NFW experiments were conducted on cotton yarn substrates. Neither EVISCN nfor EVITFAc treated yarns indicated welding to date, possibly due to high viscosities and the inability for the Poly-ILs to sufficiently wet the substrate surface. However, we are optimistic that EVITFAc has strong potential as an NFW solvent, and future experiments are ongoing.

Polyionic biocomposites were successfully prepared with both EVIEPhos and MVIMPhos using a HMPP photoinitiator and potassium persulfate thermal initiator. SEM images of the biocomposites demonstrated substantial welding and polymerization had occurred on the treated yarns. Further, imaging was conducted without sputter coating the biocomposites and did not result in charge buildup on the sample, indicating that the biocomposites were sufficiently conductive.

9. Glossary

- **μ** – Greek letter mu, a unit prefix for a factor of one millionth
- **Alkyl** – chemical group consisting of carbon and hydrogen atoms linked by only single bonds
- **Alkylation Reaction** – chemical reaction that results in the transfer of an alkyl group from one molecule to another
- **Anion** – negatively charged ion species
- **Biocomposite** – composite material consisting in some part of a material generated from a living organism
- **Biopolymer** – polymer generated by a living organism
- **Biopolymer fiber** – individual strand composed of biopolymers held by intermolecular forces
- **Biopolymer material** – material generated by a living organism typically composed of biopolymer fibers (e.g. cotton, silk, chitin, wool) organized in an organism-specific structure
- **Cation** – a positively charged ion species
- **Chaotropic** – a species that disrupts the bonding forces between other molecules
- **Cross-section** – image obtained by cutting a material, such as a yarn, perpendicular to its long axis
- **Denature** – to break apart the native structure
- **Dissolution** – process of dissolving a material in solution
- **Electrolyte** – material with ability to conduct electrical charge in the form of ions or electricity
- **Ex-situ** – polymerization of Poly-ILs outside of the biopolymer material matrix
- **Fluorescent** – property of a material to emit light in response to absorbing light
- **Halide** – negatively-charged ion from the 7th row of the periodic table (includes F^-, Br^-, Cl^-, I^-)
- **Inorganic** –compounds which are not organic (broadly, compounds not containing carbon).
- **Ion** – charged chemical species (such as Na^+, K^+, Cl^-)
- **Ionic Compound** – general classification of a chemical consisting of ions
- **Imidazolium ILs** – general chemical class of ILs based on imidazole cation structure; used in previous SC495/496 work

- **In-situ Polymerization** – polymerization of Poly-ILs within a biopolymer material matrix
- **Macromolecule** – molecule formed from a large number of atoms or smaller molecule units. Polymers are a common type of macromolecule.
- **Microcrystalline Cellulose** – processed cellulose with approximately 20% of the molecular weight of cellulose in cotton.
- **Morphology** – study of the form/structure of a material
- **NFW Solvent** – solvent capable of mobilizing biopolymers within a fiber
- **Organic –** comprised primarily from carbon and hydrogen, but may include nitrogen, oxygen and phosphorus
- **Polar** – possessing an electrical polarity (positive or negative charge)
- **Polyatomic** – chemical species consisting of more than one atom
- **Polyionic Biocomposite** – biocomposite material containing a number of charged chemical species bound in a polymer
- **Polymer** – chemical compound made of a long chain of monomer building blocks
- **Polymerizable** – property of a molecule to be able to be joined together and form a polymer
- **Radical Initiator** – chemical or light that possesses energy to cause polymerization of alkenyl monomers
- **Reactant** – starting material for a chemical reaction
- **Substituent** – any one of a number of commonly-described chemical groups in a molecule
- **Tensile strength** – bulk mechanical property of a material; a measure of resistance to break
- **van der Waals forces** – short range bonding forces that include hydrogen bonding, dipole-dipole interactions, and dispersion forces

10. References

1. Society, A. C., The Bakelizer Commemorative Booklet. ACS: Washington D.C., 1993; pp 1-5.

2. Hoff, G. P., Nylon as a textile fiber. *Ind. Eng. Chem.* **1940,** *32* (12), 1560-1564.

3. Liu, X.; Zhang, K.-Q., Silk Fiber - Molecular Formation Mechanism, Structure- Property Relationship and Advanced Applications. In *Oligomerization of Chemical and Biological Compounds*, Lesieur, C., Ed. InTech: Rijeka, 2014; p Chapter 3.

4. Byrom, D., *Biomaterials: Novel Materials from Biological Sources*. Stockton Press: New York, NY, 1991.

5. Agnarsson, I.; Kunter, M.; Blackledge, T. A., Bioprospecting finds the toughest biological material: extraordinary silk from a giant riverine orb spider. *PLOS ONE* **2010,** *5* (9), e11234.

6. Lenz, R. W., Biodegradable polymers. In *Biopolymers I. Advances in Polymer Science*, Springer, Berlin, Heidelberg: 1993; Vol. 107, pp 1-40.

7. Swatlotski, R. P.; Spear, S. K.; Holbrey, J. D.; Rogers, R. D., Dissolution of cellulose [correction of cellose] with ionic liquids. *J. Am. Chem. Soc.* **2002,** *124* (18), 4974-4975.

8. Hadadi, A.; Whittaker, J. W.; Verrill, D. E.; Hu, X.; Larini, L.; Salas-de la Cruz, D., A hierarchical model to understand the processing of polysaccharides/protein-based films in ionic liquids. *Biomacromolecules* **2018,** *19*, 3970-3982.

9. Haverhals, L. M.; Reichert, W. M.; De Long, H. C.; Trulove, P. C., Natural fiber welding. *Macromol. Mater. Eng.* **2010,** *295* (5), 425-430.

10. Haverhals, L. M.; Sulpizio, H. M.; Fayos, Z. A.; Trulove, M. A.; Reichert, W. M.; Foley, M. P.; De Long, H. C.; Trulove, P. C., Process variables that control natural fiber welding: time, temperature, and amount of ionic liquid. *Cellulose* **2012,** *19* (1), 13-22.

11. Chung, R. T.; Park, S.; Yates, E. A.; Durkin, D. P.; De Long, H. C.; Trulove, P. C., Ionic liquid property effects on the natural fiber welding process. *Electrochem. Soc. Trans.* **2018,** *86* (14), 249-255.

12. Haverhals, L. M.; Foley, M. P.; Brown, E. K.; Fox, D. M.; De Long, H. C.; Trulove, P. C., Natural fiber welding: ionic liquid facilitated biopolymer mobilization and reorganization. In *Ionic Liquids: Science and Applications*, American Chemical Society: 2012; Vol. 1117, pp 145-166.

13. Rogers, R. D.; Seddon, K. R., Ionic liquids--solvents of the future? *Science* **2003,** *302* (5646), 792-793.

14. Plechkova, N. V.; Seddon, K. R., Applications of ionic liquids in the chemical industry. *Chem. Soc. Rev.* **2008,** *37* (1), 123-150.

15. Krossing, I.; Slattery, J. M.; Daguenet, C.; Dyson, P. J.; Oleinikova, A.; Weingartner, H., Why are ionic liquids liquid? A simple explanation based on lattice and solvation energies. *J. Chem Soc. (A)* **2006,** *128* (41), 13427-13434.

16. Nie, Y.; Li, C.; Sun, A.; Meng, H.; Wang, X., Extractive desulfurization of gasoline using imidazolium-based phosphoric ionic liquids *Energy Fuels* **2006,** *20*, 2083-2087.

17. M., S. A.; A., P. M.; S., P., Molecular friction mechanisms across nanofilms of bilayer-forming ionic liquids. *J. Phys. Chem. Lett.* **2014,** *5*, 4032-4037.

18. Murakami, M.-a.; Kaneko, Y.; Kadokawa, J.-i., Preparation of cellulose-polymerized ionic liquid composite by in-situ polymerization of polymerizable ionic liquid in cellulose-dissolving solution. *Carbohydr. Polym.* **2007,** *69* (2), 378-381.

19. Zhang, H.; Wu, J.; Zhang, J.; He, J., 1-allyl-3-methylimidazolium chloride room temperature ionic liquid: a new and powerful nonderivatizing solvent for cellulose. *Macromolecules* **2005,** *38* (20), 8272-8277.

20. Trulove, P. C.; Reichert, W. M.; De Long, H. C.; Kline, S. R.; Rahatekar, S. S.; Gilman, J. W.; Muthukumar, M., The structure and dynamics of silk and cellulose dissolved in ionic liquids. *Electrochem. Soc. Trans.* **2008,** *16*, 129-139.

21. Phillips, D. M.; Drummy, L. F.; Conrady, D. G.; Fox, D. M.; Naik, R. R.; Stone, M. O.; Trulove, P. C.; De Long, H. C.; Mantz, R. A., Dissolution and regeneration of bombyx mori silk fibroin using ionic liquids. *J. Am. Chem. Soc.* **2004,** *126* (44), 14350-14351.

22. Mantz, R. A.; Fox, D. M.; Green, J. M.; Fylstra, P. A.; De Long, H. C.; Trulove, P. C., Dissolution of biopolymers using ionic liquids. *Z. Naturforsch., A: Phys. Sci.* **2007,** *62* (5-6), 275-280.

23. Wang, H.; Gurau, G.; Rogers, R. D., Ionic liquid processing of cellulose. *Chem. Soc. Rev.* **2012,** *41*, 1519-1537.

24. Visser, A. E.; Bridges, N. J.; Rogers, R. D., *Ionic liquids: science and applications*. American Chemical Society: 2012; Vol. 1117, p 0.

25. Haverhals, L. M.; Nevin, L. M.; Foley, M. P.; Brown, E. K.; De Long, H. C.; Trulove, P. C., Fluorescence monitoring of ionic liquid-facilitated biopolymer mobilization and reorganization. *Chem. Commun.* **2012,** *48*, 6417-6419.

26. Chung, R. T. *Development of Advanced Functional Biomaterials* United States Naval Academy: Annapolis, MD, 2019; p 66.

27. Fukaya, Y.; Hayashi, K.; Wada, M.; Ohno, H., Cellulose dissolution with polar ionic liquids under mild conditions: required factors for anions. *Green Chem.* **2008,** *10* (1), 44-46.

28. Xu, K.; Xiao, Y.; Cao, Y.; Peng, S.; Fan, M.; Wang, K., Dissolution of cellulose in 1-allyl-3-methylimidazolium methyl phosphonate ionic liquid and its composite system with Na_2PHO_3. *Carbohydr. Polym.* **2019,** *209*, 382-388.

29. Hirosawa, K.; Fujii, K.; Hashimoto, K.; Shibayama, M., Solvated structure of cellulose in a phosphonate-based ionic liquid. *Macromolecules* **2017,** *50* (17), 6509-6517.

30. Rumble, J. R., (Ed.), *CRC Handbook of Chemistry and Physics, 100th edition (Internet Version 2020)*. CRC Press/Taylor & Francis: Boca Raton, FL, 2020.

31. BioLogic Science Instruments, SP-300 Installation and Configuration Manual, Revision F. 2012; p 14.

32. Shreiner, R. H.; Pratt, K. W. *Standard Reference Materials: Primary Standards and Standard Reference Materials for Electrolytic Conductivity*; NIST: Washington D.C., 2004; pp 1-24.

11. Appendix

11.1 [1]H-NMR spectra of Poly -IL monomers

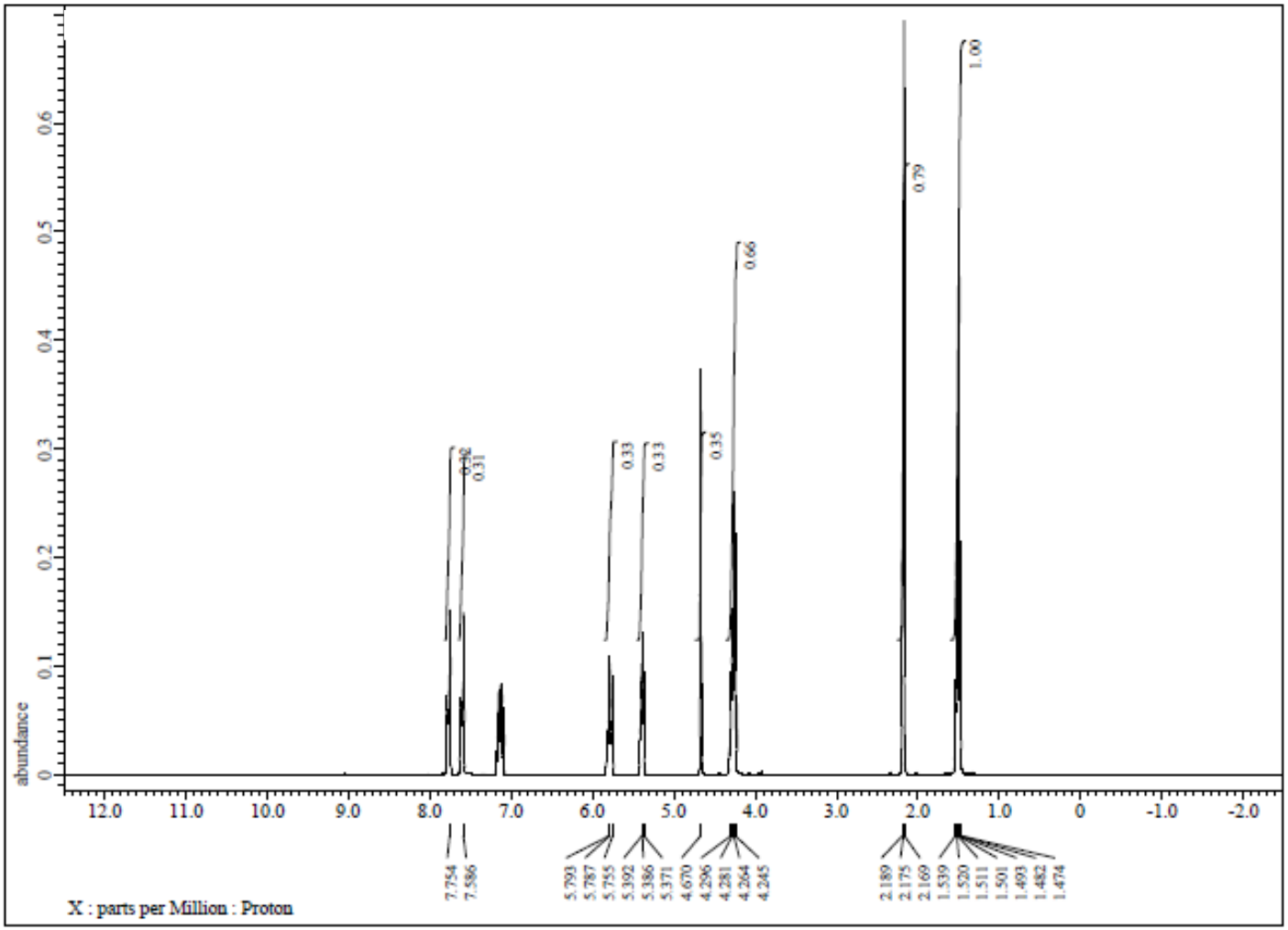

Figure A-1. [1]H-NMR of 1-ethyl-3-vinylimidazolium thiocyanate (400MHz, D_2O): 7.754 (1H, s, N^+=C**H**-N), 7.586 (1H, s, CH=C**H**-N^+), x (1H, s, N-C**H**=CH), 5.787 (1H, t, CH_2=C**H**-N), 5.386 (2H, d, C**H$_2$**=CH), 4.281 (2H, q, N^+-C**H$_2$**-CH_3), 1.520 (3H, q, CH_2-C**H$_3$**).

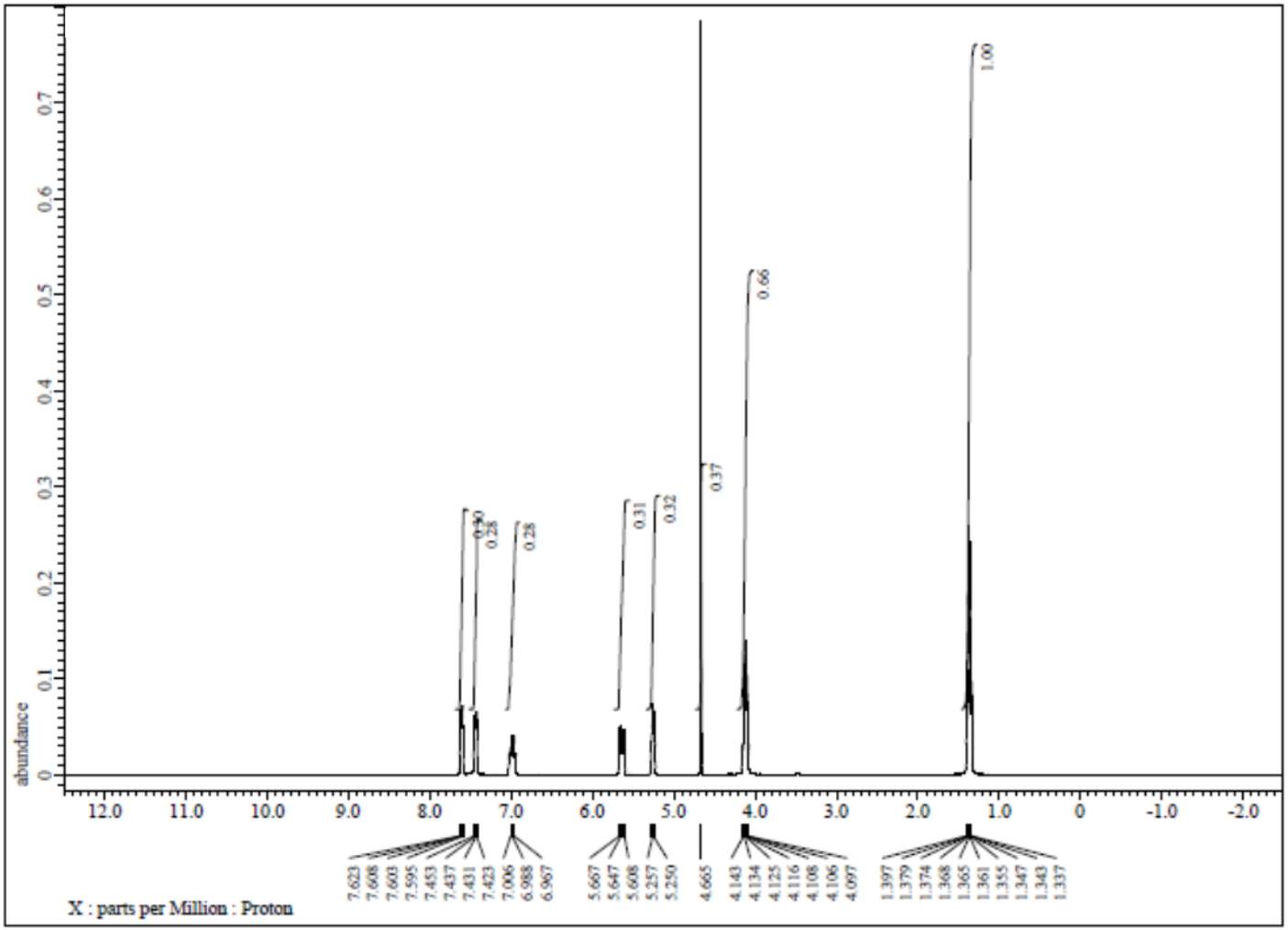

Figure A-2. ^{1}H-NMR of 1-ethyl-3-vinylimidazolium trifluoroacetate with BHT (400MHz, D_2O): 7.608 (1H, d, N^+=C**H**-N), 7.431 (1H, s, CH=C**H**-N^+), 6.988 (1H, m, N-C**H**=CH), 5.647 (1H, t, CH_2=C**H**-N), 5.257 (2H, d, C**H**$_2$=CH), 4.125 (2H, q, N^+-C**H**$_2$-CH_3), 1.365 (3H, q, CH_2-C**H**$_3$).

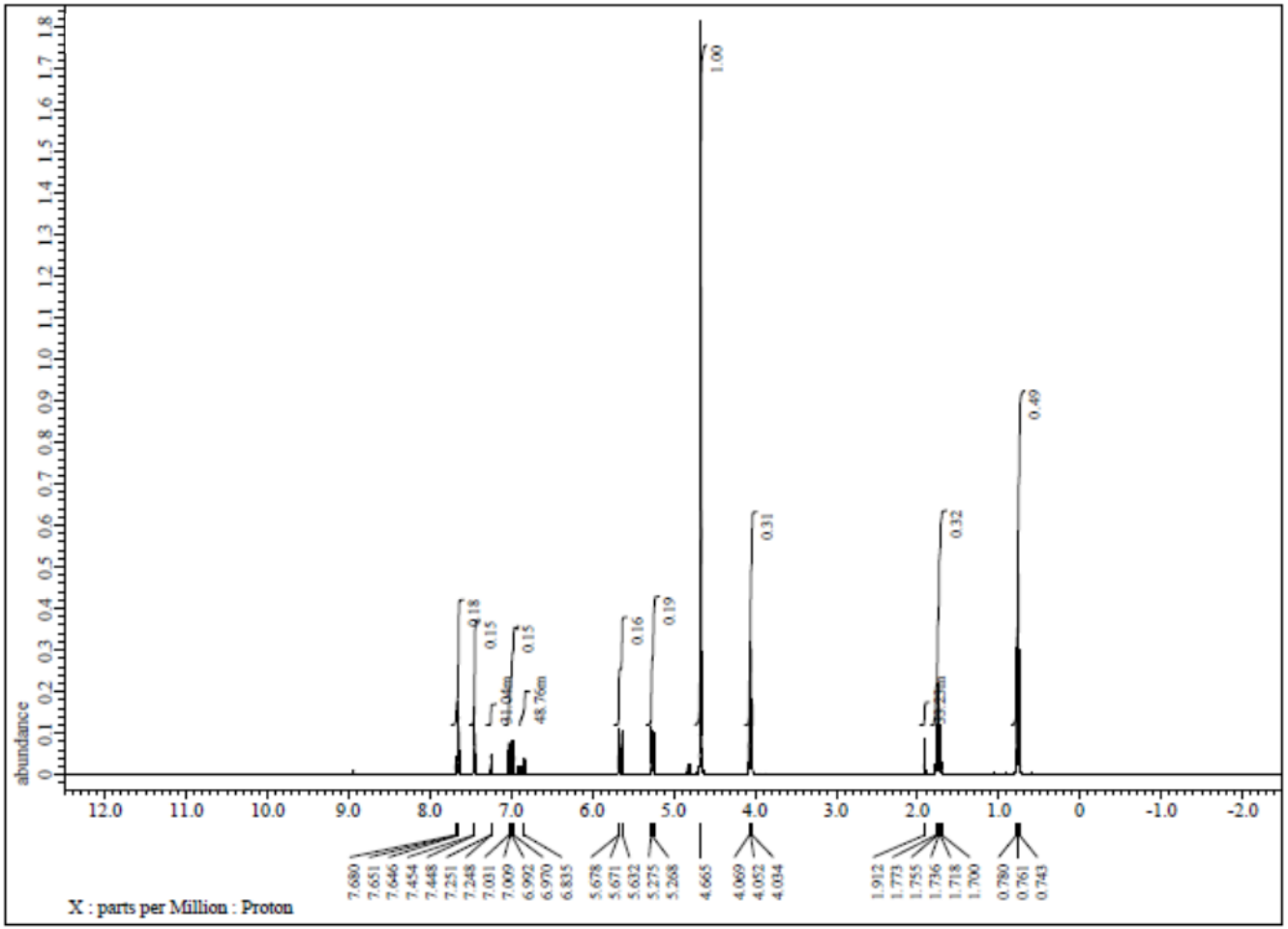

Figure A-3. ^{1}H-NMR of 1-propyl-3-vinylimidazolium chloride (400MHz, D_2O): 7.651 (1H, d, N^+=C**H**-N), 7.448 (1H, s, CH=C**H**-N^+), 7.009 (1H, m, N-C**H**=CH), 5.671 (1H, d, CH_2=C**H**-N), 5.275 (2H, d, C**H**$_2$=CH), 4.125 (2H, t, N^+-C**H**$_2$-CH_2), 1.365 (2H, m, CH_2-C**H**$_2$-CH_3), 0.761 (3H, t, CH_2-C**H**$_3$).

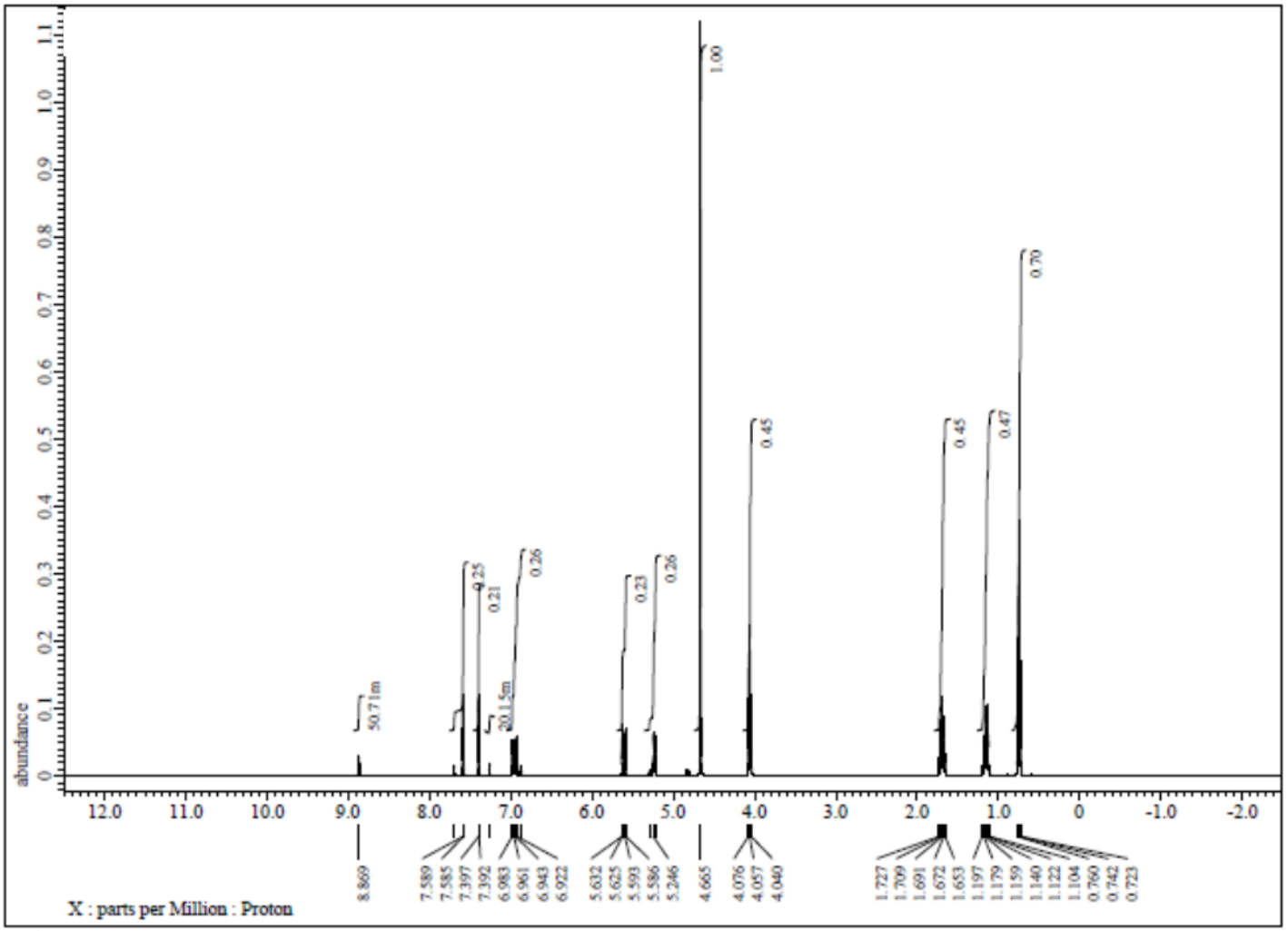

Figure A-4. ^{1}H-NMR of 1-butyl-3-vinylimidazolium chloride (400MHz, D_2O): 7.585 (1H, d, N^+=C**H**-N), 7.392 (1H, s, CH=C**H**-N^+), 6.961 (1H, m, N-C**H**=CH), 5.593 (1H, d, CH_2=C**H**-N), 5.246 (2H, d, C**H$_2$**=CH), 4.057 (2H, t, N^+-C**H$_2$**-CH_2), 1.691 (2H, m, CH_2-C**H$_2$**-CH_2), 1.140 (2H, m, CH_2-C**H$_2$**-CH_3), 0.742 (3H, m, CH_2-C**H$_3$**).

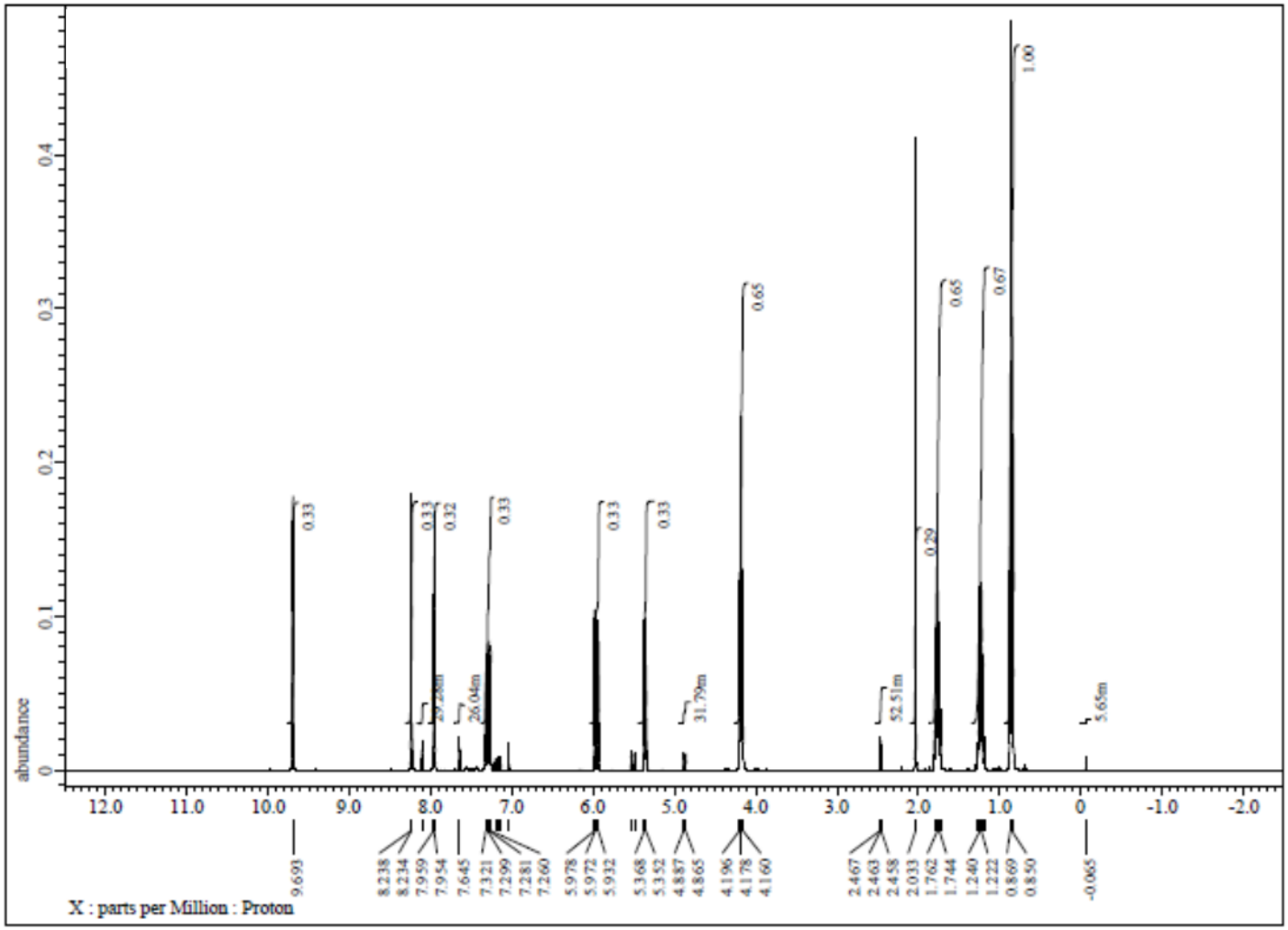

Figure A-5. ^{1}H-NMR of 1-butyl-3-vinylimidazolium trifluoroacetate (400MHz, DMSO-d_6): 8.234 (1H, d, N^+=C**H**-N), 7.954 (1H, s, CH=C**H**-N^+), 7.299 (1H, m, N-C**H**=CH), 5.972 (1H, d, CH_2=C**H**-N), 5.352 (2H, d, C**H$_2$**=CH), 4.178 (2H, t, N^+-C**H$_2$**-CH_2), 1.762 (2H, m, CH_2-C**H$_2$**-CH_2), 1.240 (2H, m, CH_2-C**H$_2$**-CH_3), 0.869 (3H, m, -CH_2-CH_2-C**H$_3$**).

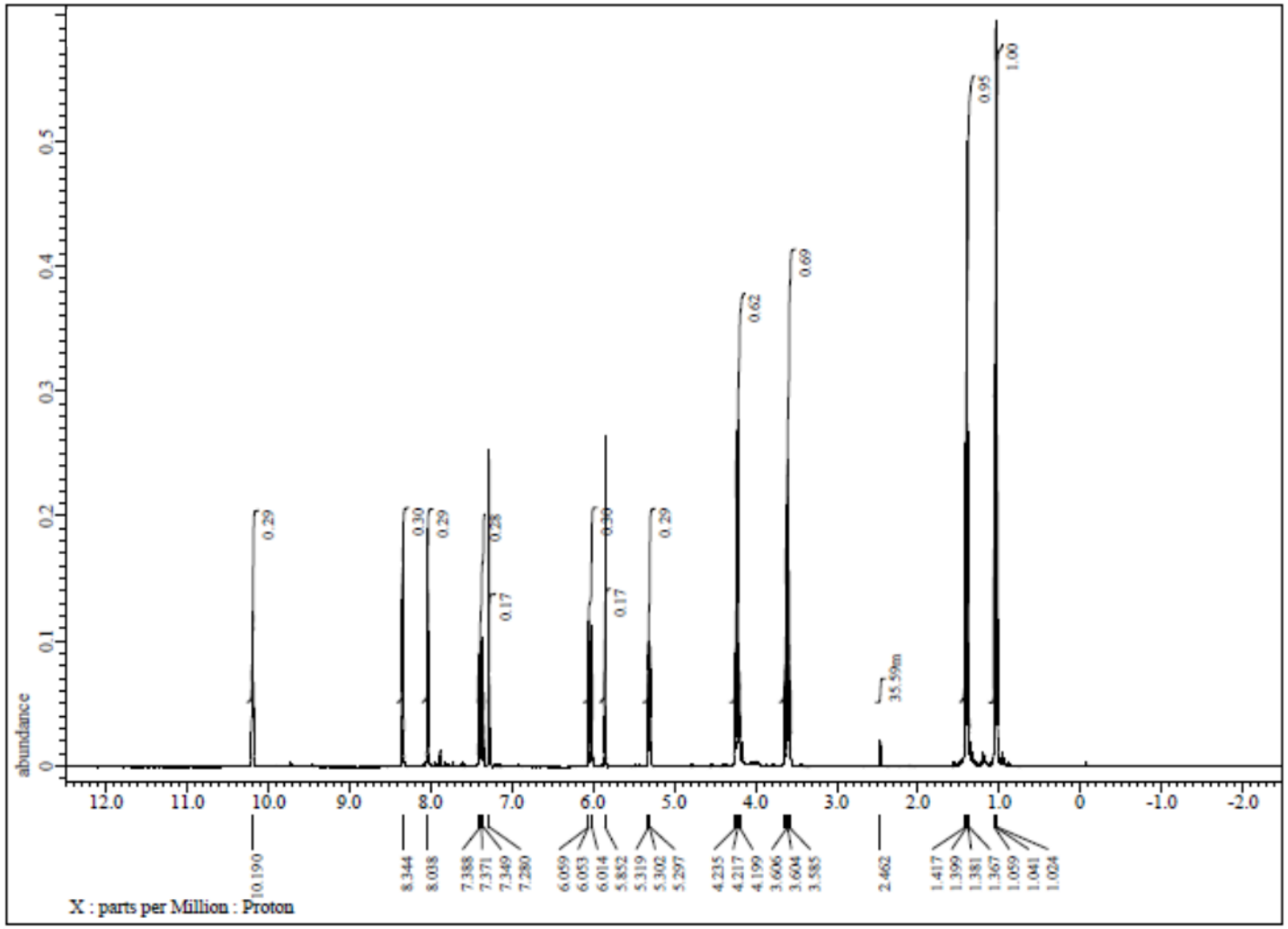

Figure A-6. ^{1}H-NMR of 1-ethyl-3-vinylimidazolium ethylphosphonate (400MHz, DMSO-d_6): 10.190 (1H, s, P-**H**), 8.344 (1H, s, N^+=C**H**-N), 8.038 (1H, s, CH=C**H**-N^+), 8.038 (1H, s, N-C**H**=CH), 5.302 (1H, t, CH_2=C**H**-N), 5.257 (2H, d, C**H**$_2$=CH), 4.127 (2H, q, N^+-C**H**$_2$-CH_3), 3.604 (2H, m, P-C**H**$_2$-CH_3) 1.365 (3H, t, N^+-CH_2-C**H**$_3$), 1.041 (3H, t, P- P-CH_2-C**H**$_3$)

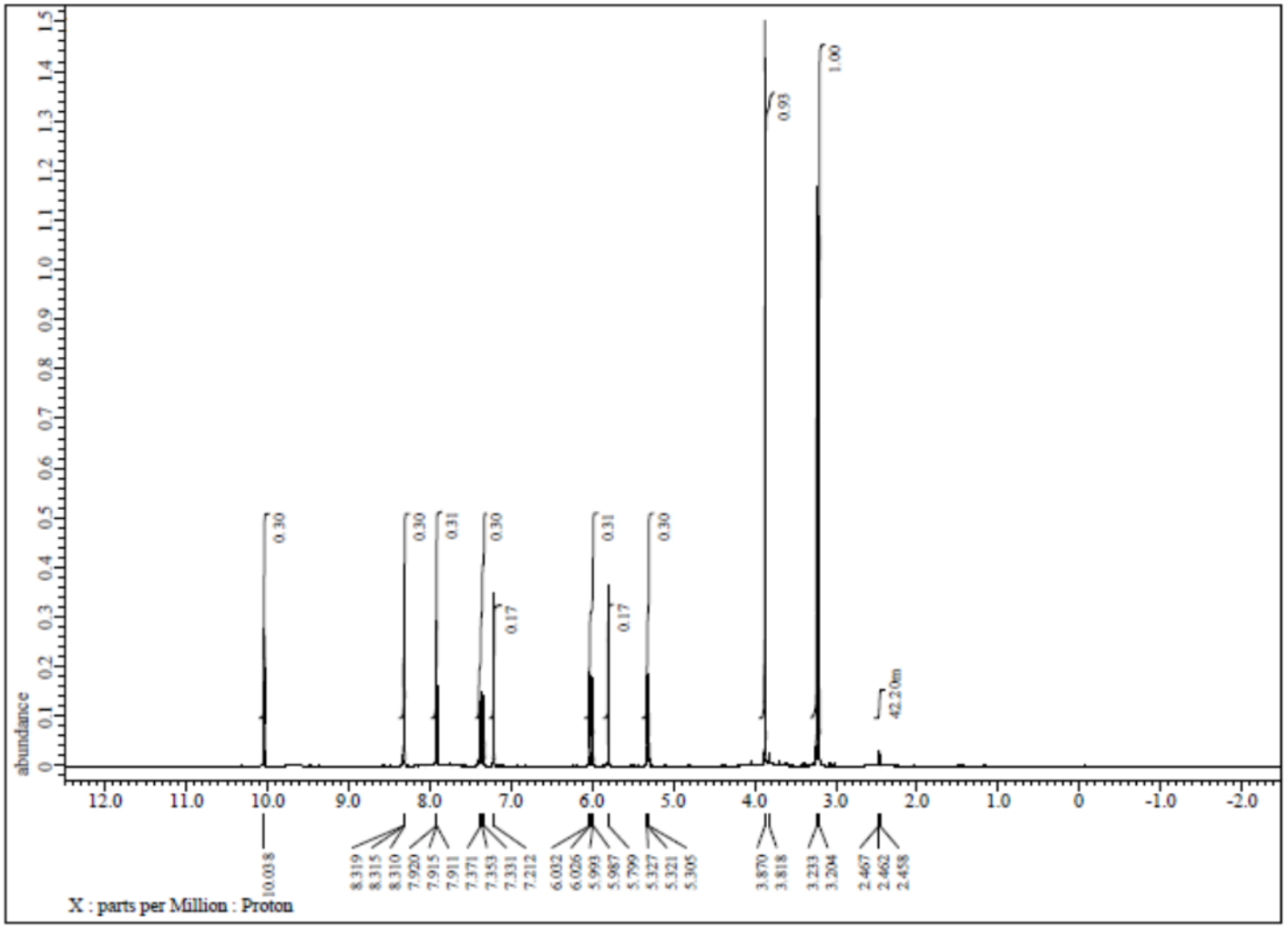

Figure A-7. ^{1}H-NMR of 1-methyl-3-vinylimidazolium methylphosphonate (400MHz, DMSO-d_6): 8.315 (1H, s, N^+=C**H**-N), 7.915 (1H, s, CH=C**H**-N^+), 7.353 (1H, m, N-C**H**=CH), 7.212 (1H, s, CH_2=C**H**-N), 5.993 (1H, d, C**H₂**=CH), 5.799 (1H, s, P-**H**), 5.321 (1H, d, C**H₂**=CH), 3.870 (2H, q, N^+-C**H₃**), 3.233 (3H, m, P-C**H₃**)

11.2 DFT Calculations

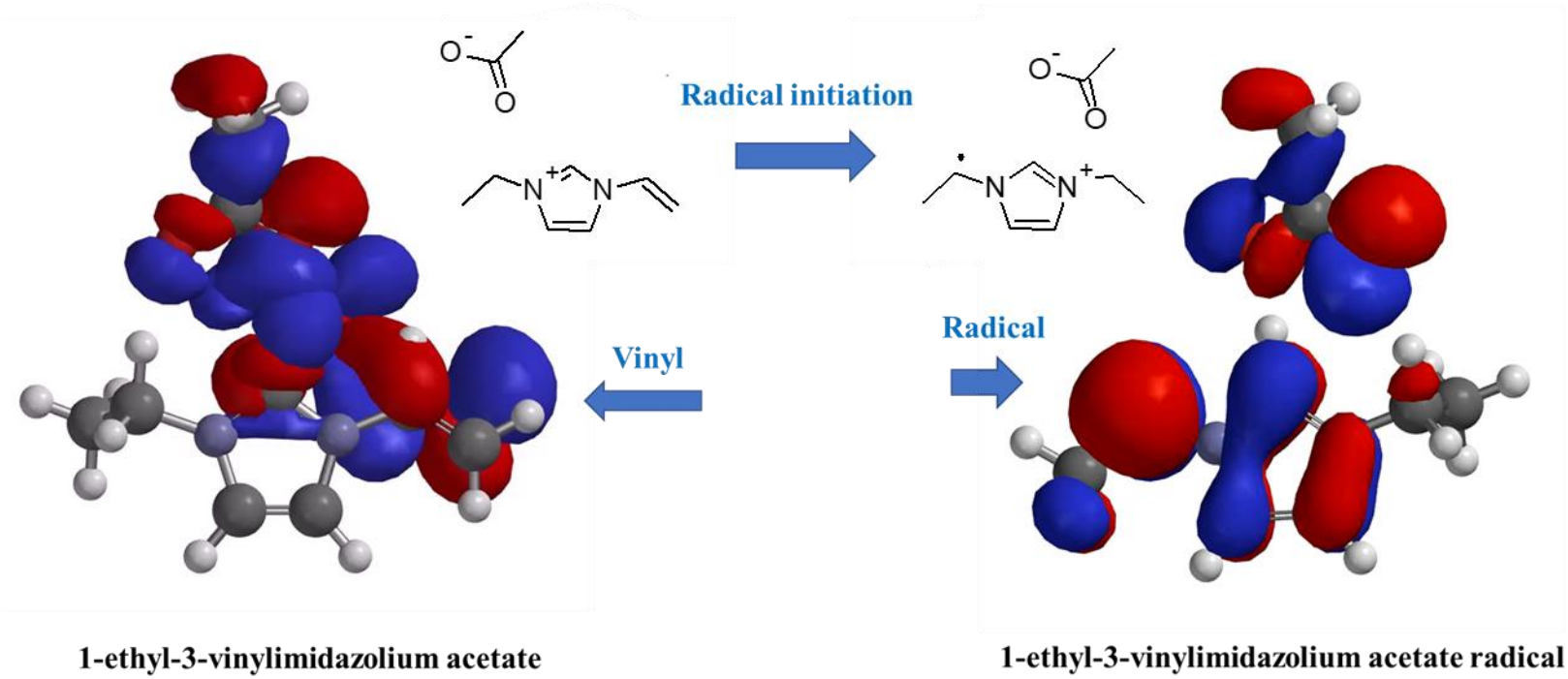

Figure A-8. Ball and stick model of DFT calculations illustrating the LUMO orbitals of the EVIAc monomer and HOMO orbitals of the resulting EVIAc radical. Coloration indicates whether the orbital phase is positive (blue) or negative (red).

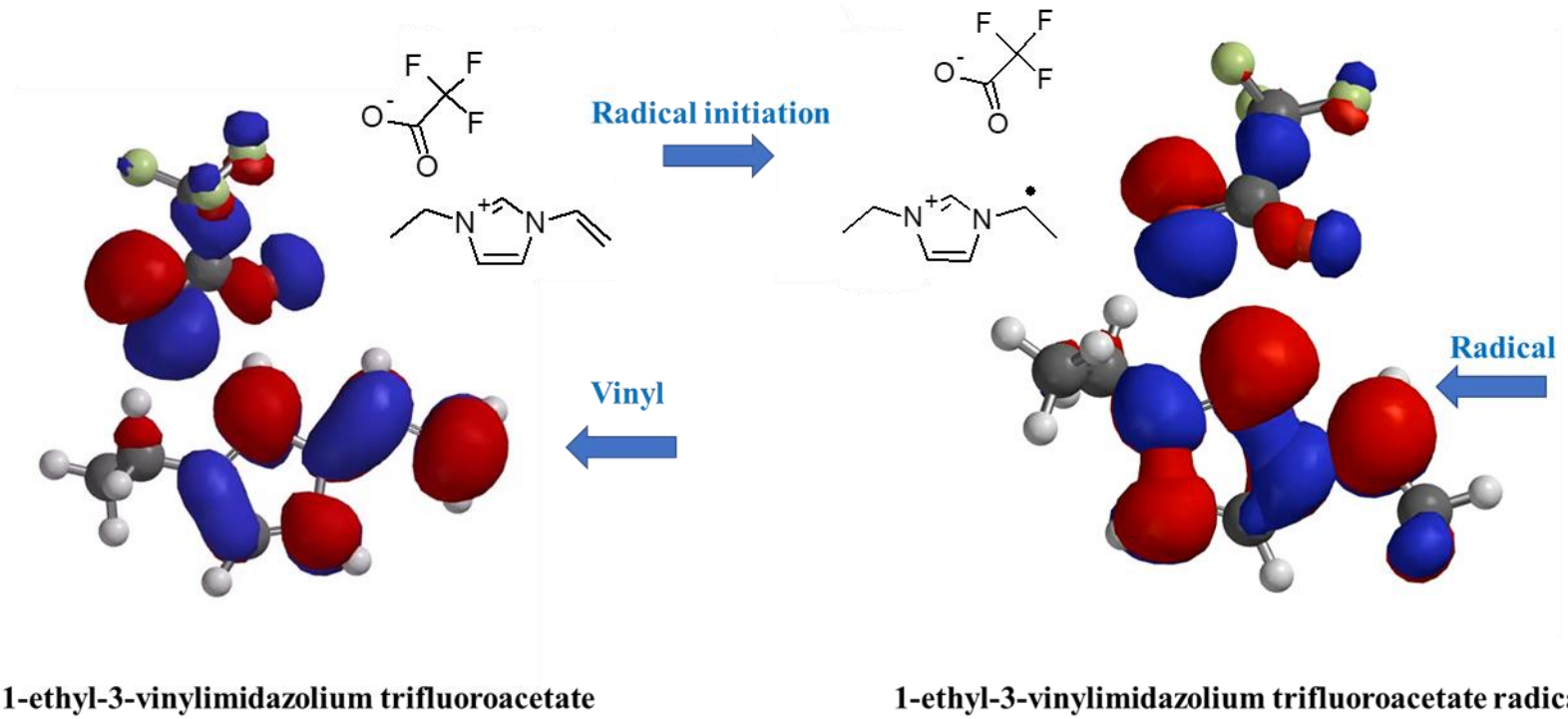

Figure A-9. Ball and stick model of DFT calculations illustrating the LUMO orbitals of the EVITFAc monomer and HOMO orbitals of the resulting EVITFAc radical. Coloration indicates whether the orbital phase is positive (blue) or negative (red).

11.3 [1]H-NMR spectra of polymerized Poly -ILs

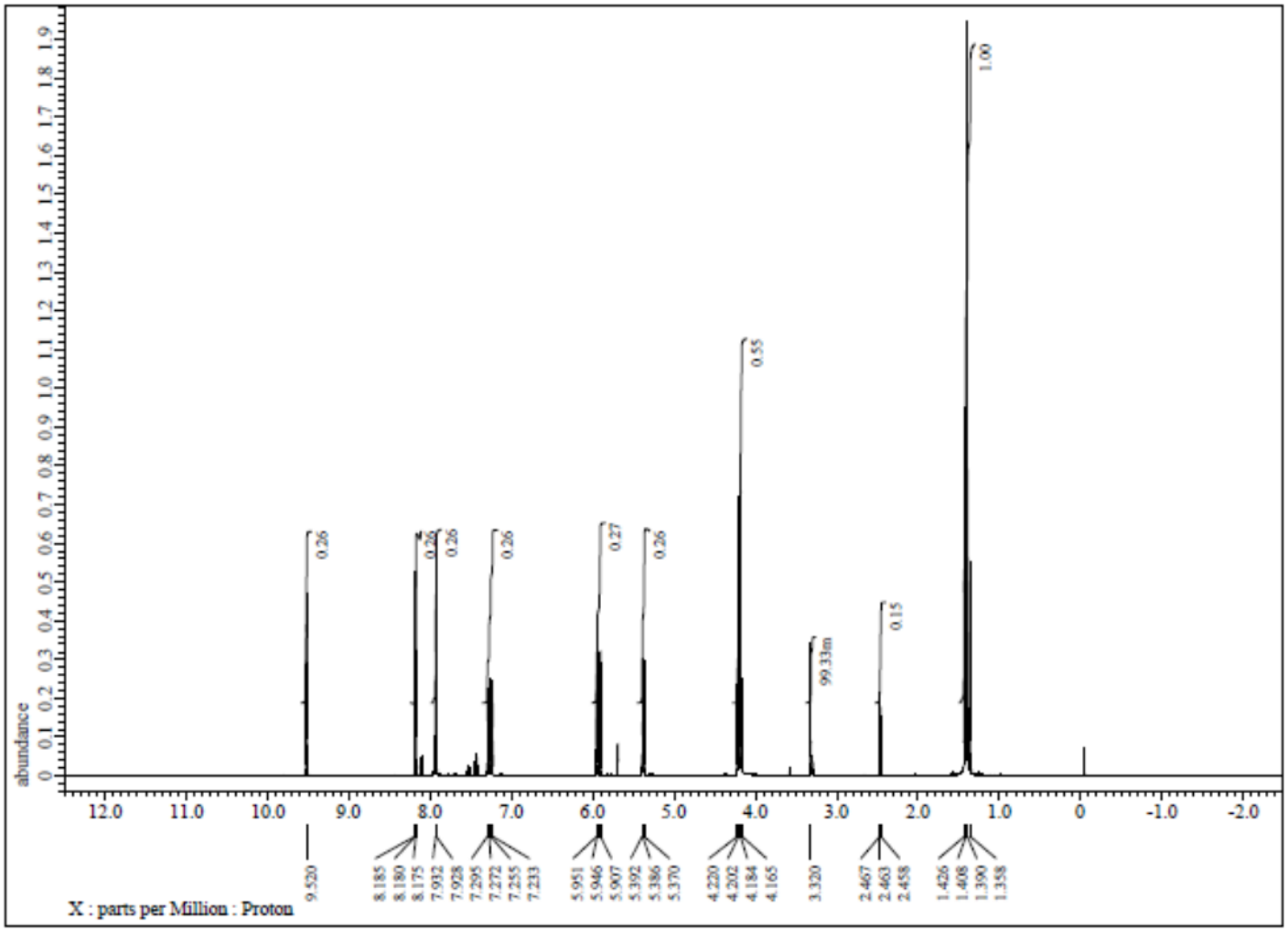

Figure A-10. [1]H-NMR of poly-[1-ethyl-3-vinylimidazolium trifluoroacetate] with BHT (400MHz, D_2O): 7.608 (1H, d, N^+=C**H**-N), 7.431 (1H, s, CH=C**H**-N^+), 6.988 (1H, m, N- C**H**=CH), 5.647 (1H, t, CH_2=C**H**-N), 5.257 (2H, d, C**H₂**=CH), 4.125 (2H, q, N^+-C**H₂**-CH_3), 1.365 (3H, q, CH_2-C**H₃**)

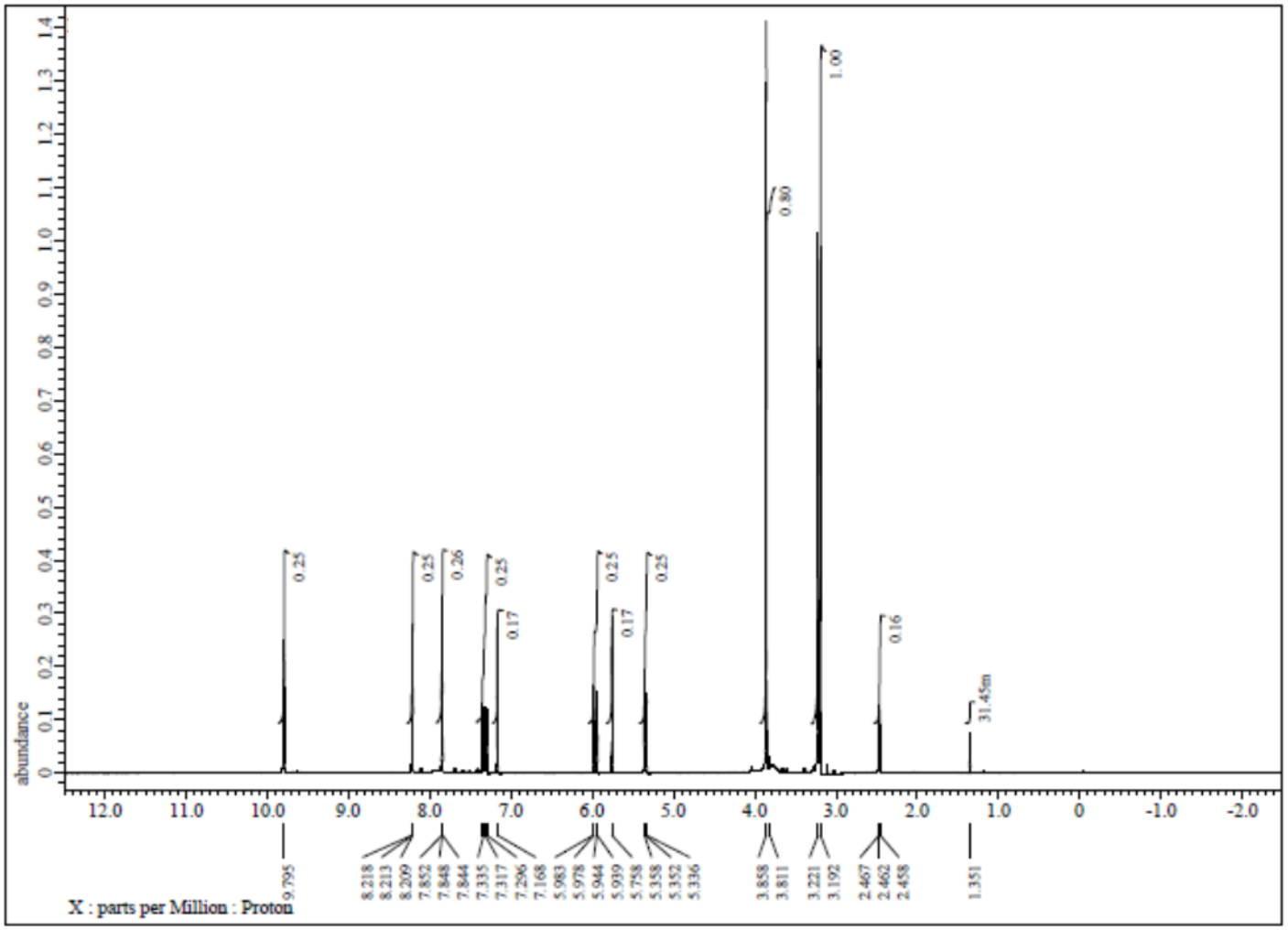

Figure A-11. ^{1}H-NMR of poly-[1-methyl-3-vinylimidazolium methylphosphonate] (400MHz, DMSO-d_6): 8.213 (1H, s, N^+=C**H**-N), 7.848 (1H, s, CH=C**H**-N^+), 7.317 (1H, m, N-C**H**=CH), 7.168 (1H, s, CH_2=C**H**-N), 5.944 (1H, d, C**H**$_2$=CH), 5.758 (1H, s, P-**H**), 5.352 (1H, d, C**H**$_2$=CH), 3.858 (2H, q, N^+-C**H**$_3$), 3.221 (3H, m, P-C**H**$_3$)

11.4 Electrochemical Impedance Spectroscopy (EIS)

An electrochemical cell was prepared by placing four, 3-inch long (ca. 1 mm diameter) platinum electrodes into wells cut onto a Teflon sheet. The platinum leads were equally spaced at approximately 0.3 cm over a distance of 1.5 cm. A BioLogic SP-300 potentiostat was connected to the platinum leads in a four-electrode measurement configuration (Figure A-12) in accordance to the SP-300 manual.[31] Calibration and initial testing was conducted using solutions of KCl and $CaCl_2$. Solutions of KCl (1 M, 0.1 M, and 0.01 M) were prepared via serial dilution, while $CaCl_2$ solutions (10 wt%, 5 wt%, and 1 wt%) were prepared gravimetrically. Solutions were placed directly onto the electrodes, ensuring coverage of all four electrodes. Measurements were conducted using EC-Labs software using the potentiometric electrochemical impedance spectroscopy (EIS) settings. Between measurements electrodes were rinsed with ultrapure water.

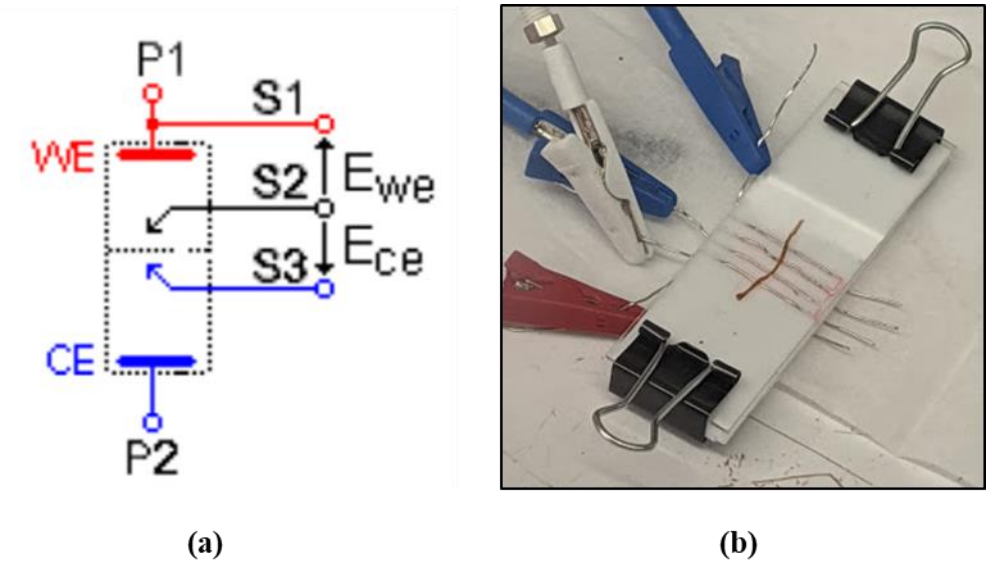

Figure A-12. (a) Four electrode configuration for BioLogic SP-300 Potentiostat, and (b) custom designed measurement cell.

Calibration and initial testing of the prepared measurement cell resulted in inconsistent measurements with deviations from the literature values[30, 32] (Figure A-13 and Figure A-14).

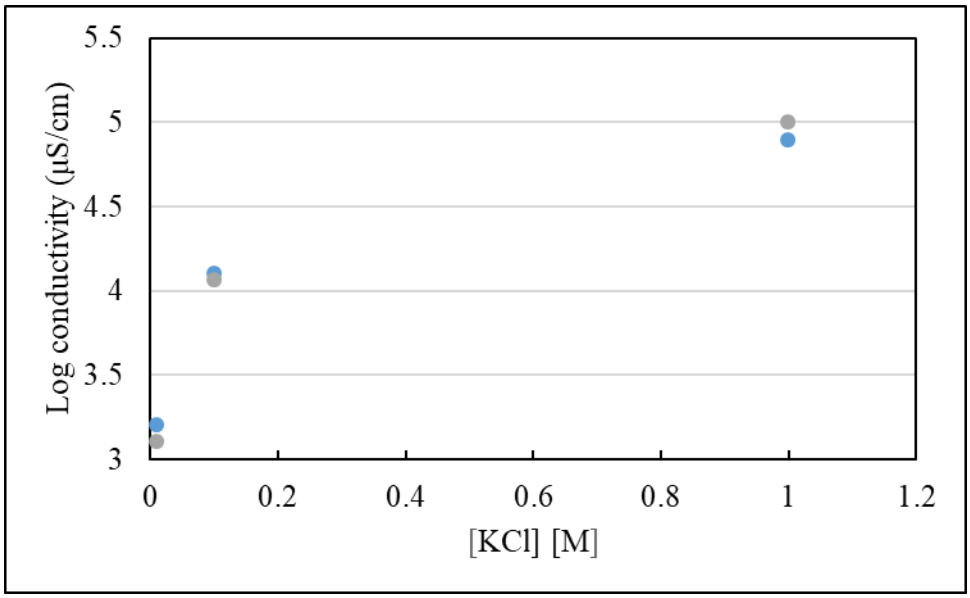

Figure A-13. Plot of EIS four-electrode measurements for KCl (blue) and NIST literature values (grey).

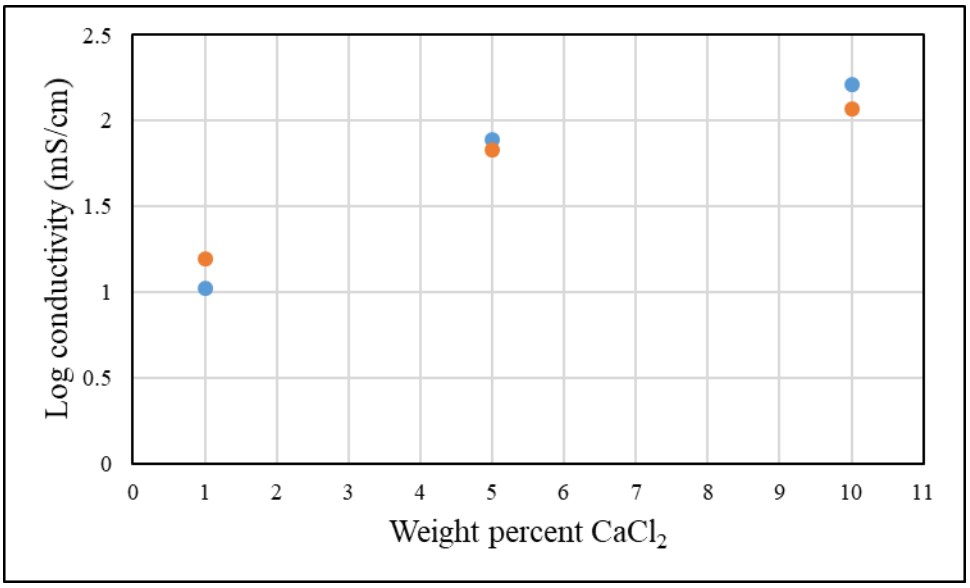

Figure A-14. Plot of EIS four-electrode measurements for $CaCl_2$ (blue) and CRC literature values (orange).

Deviations between the experimental and literature values were inconsistent between solutions of different concentration or weight percentage, which negates the ability to calculate a specific cell constant. Further, while repeated measurements of samples provided reproducible results, analyzing different samples of the same solution required multiple measurements before resulting in reproducible results.

However, the measurements do demonstrate significant changes between solutions of different concentration and weight percent. These results indicate the prepared measurement cell and technique parameters may be adequate for determining relative changes in conductivity among various polyionic biocomposites. Further investigation into this technique may yield the ability to determine the effect of changing synthesis parameters or environmental conditions on the conductivity of polyionic biocomposites.